공학박사 학위논문

# Enhanced therapeutic angiogenesis in mouse hindlimb ischemia model by electrical stimulation and extracellular matrix

# 전기 자극과 세포외 기질을 이용한 마우스 하지 허혈 모델에서의 혈관 재생 향상

2018년 2월

서울대학교 공과대학

화학생물공학부

정 근 재

# Abstract

# Enhanced therapeutic angiogenesis in mouse hindlimb ischemia model by electrical stimulation and extracellular matrix

**Gun-Jae Jeong**

**School of Chemical and Biological Engineering**

**The Graduate School**

**Seoul National University**

The present study is the report on the enhancing therapeutic angiogenesis in mouse hindlimb ischemia model by usage of electrical stimulation (ES) derived from solar cell and injectable decellularized extracellular matrix (IDM) for stem cell transplantation. In ischemic tissue, most of the transplanted cells and native cells undergo apoptosis and necrosis due to the low oxygen and nutrient delivery. Therefore, improved cell therapy method of acellular therapy method is required for enhancing or replacing previous therapy.

In chapter 3, the solar-cell-based device was designed, which converts light energy to electrical energy, can generate an electrical stimulus that would control cell behavior and stimulate therapeutic angiogenesis in a mouse ischemic hindlimb. For easy utilization of the device *in vivo*, we designed a solar cell circuit that consisted of an implantable electrode and a solar panel that adhered to the skin. Conventional clinical ES usually involves a large electrical device, which may require patient hospitalization. By contrast, the solar-cell-based wearable device developed in this study overcomes the limitation. In an *in vitro* experiment, ES applied to various types of cells associated with angiogenesis significantly enhanced cell migration and secretion of angiogenic paracrine factors. To evaluate the therapeutic efficacy of the device *in vivo*, the electrode of the solar cell device was implanted into the ischemic region of a mouse hindlimb, and the solar panel part of the device was attached to the back of mouse for exposure to light. The device successfully converted light energy into electrical energy and generated ES. ES induced cell migration and promoted the secretion of angiogenic paracrine factors. Furthermore, use of the solar cell device led to significant increase in the number of capillaries and arterioles at the ischemic region, and prevented muscle necrosis and loss of the ischemic limb.

In the chapter 4, IDM was investigated and examined whether the IDM can enhance transplanted cell grafting and therapeutic efficacy. In an *in vitro* experiment, IDM and ADSC complex (cell-IDM) enhanced cell viability and upregulation of angiogenic paracrine factors. To evaluate the therapeutic efficacy *in vivo*, cell-IDM was implanted into the ischemic region of a mouse hindlimb. Transplantation of cell-IDM induced significant increase in the number of capillaries and arterioles at the ischemic region, and prevented muscle necrosis.

The result of this study may be applicable for the enhancing and optimizing therapeutic angiogenesis in both cell transplantation model and *in vivo* implantable device model. Moreover, this study provided a disposable and easily usable and implantable ES-generating solar cell device and easily applicable developed stem cell transplantation method to treat angiogenic disease.

**Keywords : angiogenesis, ischemic disease, stem cell transplantation, solar cell, decellularized matrix, extracellular matrix**

***Student Number* : 2012-20973**

# Table of contents

# List of figures

# Abbreviations

| | |
|---|---|
| ADSC | adipose derived stem cell |
| BM | bone marrow |
| Cell-IDM | IDM-hADSC complex |
| CLI | critical limb ischemia |
| DAPI | 4',6-diamidino-2-phenylindole |
| DMEM | dulbecco's modified eagle's medium |
| EB | ethidium bromide |
| ECM | extracellular matrix |
| EF | electrical field |
| EPC | endothelial progenitor cell |
| ES | electrical stimulation |
| FBS | fetal bovine serum |
| FDA | fluorescein diacetate |

| | |
|---|---|
| FGF | fibroblast growth factor |
| H&E | hematoxylin and eosin |
| HNA | human nuclear antigen |
| HSC | hematopoietic stem cell |
| IDM | injectable decellularized matrix |
| ITO | indium tin oxide |
| MACS | magnetic-activated cell sorting |
| mEC | mouse endothelial cells |
| mEPC | mouse endothelial progenitor cells |
| mMSC | mouse mesenchymal stem cells |
| mMyoblast | mouse myoblasts |
| MSC | mesenchymal stem cell |
| P3HT | poly(3-hexylthiophene) |
| PAD | peripheral arterial disease |
| PBS | phosphate buffered saline |

| | |
|---|---|
| PCBM | phenyl-C61-butyric acid methyl ester |
| PI | polyimide |
| PI | propidium iodide |
| SDS-PAGE | sulfate–polyacrylamide gel electrophoresis |
| SM α-actin | smooth muscle α-actin |
| TGF | transforming growth factor |
| VEGF | vascular endothelial growth factor |
| ZnO | zinc oxide |

# Chapter 1.
# Research backgrounds and objective

## 1.1 Angiogenesis

Angiogenesis is the growth of blood vessels from the existing vasculature. Every metabolically active tissue in the body is exist nearby blood vessels. These blood vessels are formed by the process of angiogenesis. Blood vessels are needed in all tissues for exchange of nutrients and metabolites. Small blood vessels are consist of endothelial cells, and the larger vessels are supported by mural cells such as smooth muscle cells. Vasculogenesis is the process of blood vessel formation by endothelial progenitors, whereas the angiogenesis and artheriogenesis is the process of mural cell sprouting and stabilization. When metabolic activity of certain tissue changed, there are proportional changes in angiogenesis and proportional changes occurs in vessel. In this regulation oxygen plays a pivotal role. Hemodynamic factors are critical for survival of vascular networks and for structural adaptations of vessel walls. Once the vessel system is mismanaged, the body impact the unexpected disorders including cancer, arthritis, blindness, ischemic disease, etc. Recent researches on blood vessels enabled us to have better understanding on vessel growth and advanced therapeutic approaches on treating blood vessel disorders.

Decreasing or inhibiting angiogenesis can be therapeutic in cancer, ophthalmic conditions, rheumatoid arthritis, and other diseases. Capillaries grow and regress in healthy tissues according to functional demands. Exercise stimulates angiogenesis in skeletal muscle and heart. A lack of exercise leads to capillary regression. Capillaries grow in adipose tissue during weight gain and regress during weight loss. Clearly, angiogenesis occurs throughout life.

Angiogenic factors and inhibitors have been discovered only in the past decade, the elucidation of their interactions with each other is only beginning to be uncovered.[1] Numerous inducers of angiogenesis have been identified, including the members of the vascular endothelial growth factor (VEGF) family, angiopoietins, transforming growth factors (TGF), platelet-derived growth factor, tumor necrosis factor-α, interleukins and the members of the fibroblast growth factor (FGF) family.[2-3] In addition, many factors control and influence angiogenesis including soluble growth factors, membrane-bound proteins, cell–matrix and cell–cell interactions, and many interacting systems[2].

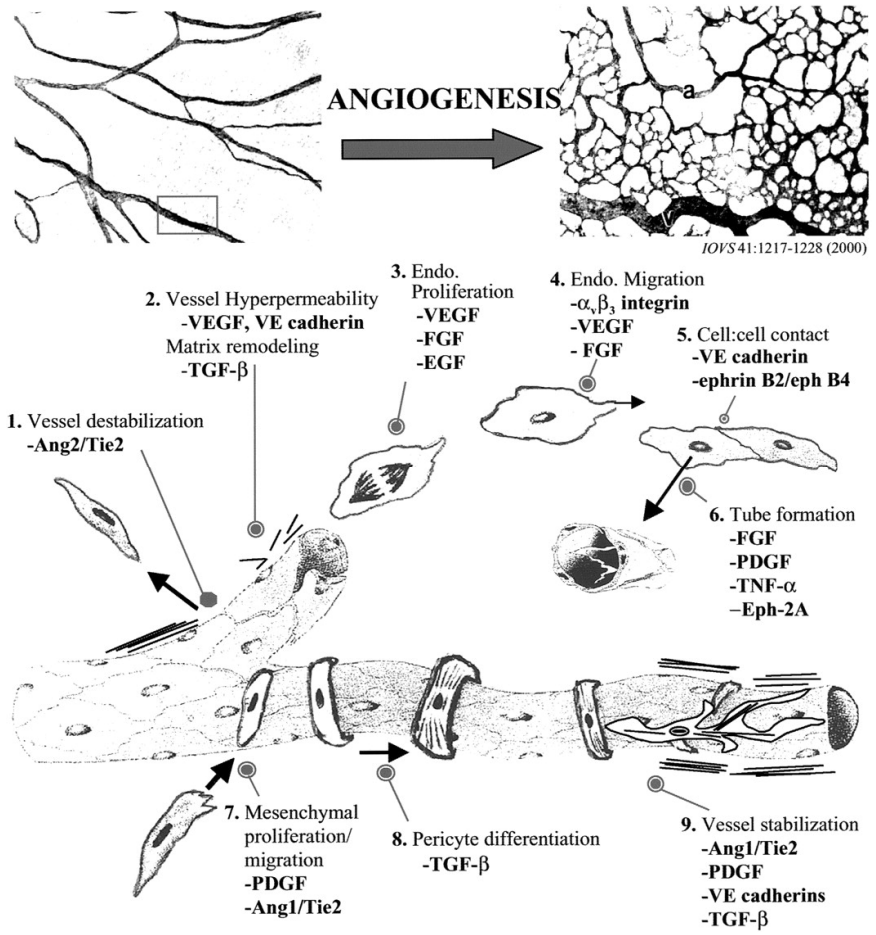


**Figure 1.1. Mechanisms of physiological angiogenesis[4]**

## 1.2 Ischemic disease and cell therapy

Peripheral arterial disease (PAD) and Buerger's disease are the disorders combining pain, ulcerations and damagers or gangrene of finger or toes by narrowed and blocked peripheral arteries in hands and feet.[5-6] The patients are given a diagnosis of critical limb ischemia (CLI). Despite of the medical advances in limb perfusion treatments, still high rate of limb amputation and mortality is observed. For a recent decade, cell-based therapy has been a seemly option for CLI therapeutic improvement.[7] Cell therapy can offer neovascularization, cell recruitment for tissue regeneration via inducement and several cytokines such as pro-angiogenic and pro-survival factor for tissue protection and remodeling.[8-10] For ischemic diseases, stem cells such as mesenchymal stem cells (MSCs), adipose-derived stem cells (ADSCs), and hematopoietic stem cells (HSCs) have been isolated and transplanted to the damaged tissues, and paracrine factors release from the cells are considered as the essential component which can stimulate angiogenesis.[11] However, there is a major hurdle to apply the cell therapies on ischemic diseases, and it is low survival rate at an ischemic tissue environment with low oxygen levels, glucose and pH, accompanied by the lack of blood supply.[5] The poor survival rate of

transplanted cells need to be improved for the clinical applications. The major concerns on cell transplantation therapy are the engraftment and survival of delivered cells, which are prerequisites and determinants of clinical efficiencies.[12-13] However, most of the injected cells undergo apoptosis in a few days without successful integration with host tissues[14], and the number of survived cells would not be enough to induce angiogenesis. For these reasons, excessive populations of cells become necessary, and cells should be cultured an expanded *in vitro*. Unfortunately, this means that patients would not be able to get a direct isolation-to-transplantation treatment and additional time and costs would be incurred during expansion culture period.

## 1.3. Electrical stimulation on therapeutic angiogenesis

Electrical stimulation (ES) has been suggested to be a promising approach for regenerating tissue, which can overcome the limitations of conventional stem cell therapy.[15-18] Endogenous electrical field (EF) is generated in the vasculature when angiogenesis occurs, which is generated by active ion transport across endothelium.[19] A previous study demonstrated that ES of the ischemic region resulted in strong upregulation of the expression of VEGF by skeletal muscle cells, and significantly enhanced angiogenesis for tissue regeneration (Figure 1.2).[16] Another study demonstrated that ES promoted the reorientation and migration of endothelial cells *in vitro*, which was mediated through PI3K-Akt/Rho-ROCK signaling pathways and reorganization of the actin cytoskeleton.[20] When skin is injured, a transepithelial potential difference develops at the layer of skin tissue, and the potential difference induces an electrical field at the wound, which persists until re-epithelialization is complete.[21] The endogenous EF induces migration of epithelial cells toward the wound in order to regenerate tissue, and wound healing is compromised when the endogenous EF is inhibited.[22] Although EF in wound healing has recently

been studied[23], the role of ES or EF in therapeutic angiogenesis and subsequent tissue repair for ischemic diseases has not been clearly elucidated. ES was previously shown to direct the behavior of cells involved in the healing wounds.[22]

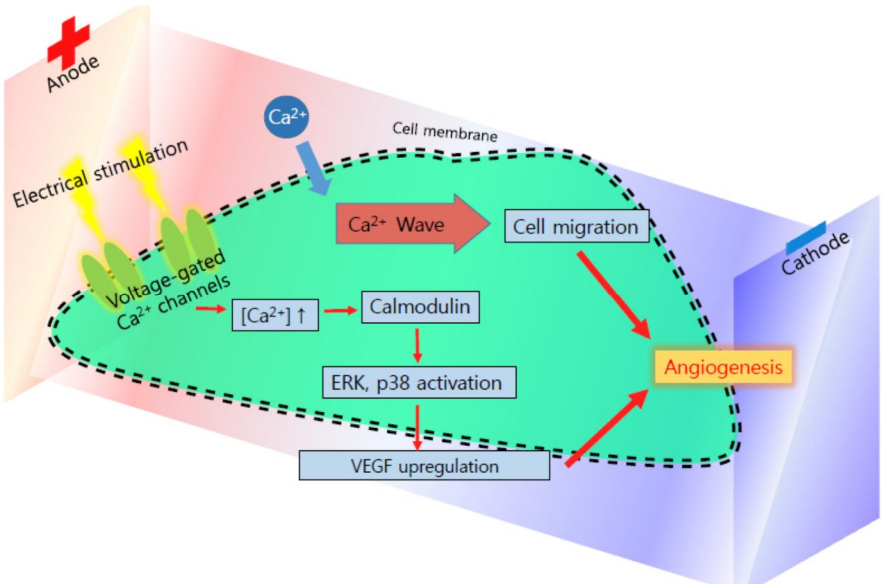


**Figure 1.2.** Intracellular angiogenesis mechanism of electrical stimulation

## 1.4. Extracellular matrix (ECM)

All cells make close contact with the ECM, either continuously or at important phases of their lives (for instance, as stem or progenitor cells or during cell migration and invasion). The ECM is well known for its ability to provide structural support for organs and tissues, for cell layers in the form of basement membranes, and for individual cells as substrates for migration. The role of the ECM in cell adhesion and signaling to cells through adhesion receptors such as integrins has received much attention[24-26], and, more recently, mechanical characteristics of the matrix (stiffness, deformability) have also been recognized to provide inputs into cell behavior.[27-28] Thus, ECM proteins and structures play vital roles in the determination, differentiation, proliferation, survival, polarity, and migration of cells. ECM signals are arguably at least as important as soluble signals in governing these processes. Many growth factors (e.g., FGF and VEGF) bind avidly to heparin and to heparin sulfate, a component of many ECM proteoglycans (PGs). Hence, a generally held view is that heparan sulfate PGs act as a sink or reservoir of growth factors and may assist in establishing stable gradients of growth factors bound to the ECM; such gradients of morphogens play vital roles in patterning

developmental processes. It is also often proposed that growth factors can be released from the ECM by degradation of ECM proteins or of the glycosaminoglycan components of PGs. Those models place the ECM in a distal role, acting as localized reservoirs for soluble growth factors that will be released from the solid phase to function as traditional, soluble ligands. There are also increasing numbers of examples of growth factors binding to ECM proteins themselves, without the involvement of glycosaminoglycans, supporting the notion that the presentation of growth factor signals by ECM proteins is an important part of ECM function.

## 1.5. Improvement cell transplantation therapy

To improve the survival and engraftment of transplanted stem cells in ischemic tissue, several strategies have been developed. These strategies incorporate transplantation in preconditioning of stem cells[29-30], genetic modifications of stem cells[29, 31-32], combination with growth factors delivery[33], and the application of tissue engineering scaffolds[34]. While preconditioning of stem cells for transplantation has higher efficacy, it has certain limitations. Because he stem cells can be damaged and differentiated in preconditioning step, several issues should be addressed before clinical tials.[29] Genetic modifications of stem cells have problems such as low efficiency of transfection, mutagenic potential of target genes, and cytotoxicity.[35-36] Growth factor delivery with cell transplantation can enhance the survival of stem cells, but a controlled release system must be developed to avoid side effects and protract growth factor activity in vivo.[37]

In terms of tissue engineering, synthetic analogs or biologically derived ECM can be used as an appropriate cell carrier for transplantation. These can provide a substrate to transplanted cell adhesion and serve as a scaffold

for tissue repair to exogenous and resident cells.[38-39] Several studies reported that cell transplantation with hydrogel containing ECM components enhanced therapeutic efficacy in myocardial infarction, limb ischemia, and bone regeneration model.[40-42]

## 1.6. Research objective of thesis

The research objective in this thesis is the enhancing therapeutic angiogenesis in mouse hindlimb ischemia model by usage of electrical stimulation derived from solar cell and injectable decellularized extracellular matrix (IDM).

Firstly, the chapter 3 reports the solar-cell-based device, which converts light energy to electrical energy, can generate an electrical stimulus that would control cell behavior and stimulate therapeutic angiogenesis in a mouse ischemic hindlimb. For easy utilization of the device *in vivo*, we designed a solar cell circuit that consisted of an implantable electrode and a solar panel that adhered to the skin. Conventional clinical ES usually involves a large electrical device, which may require patient hospitalization. By contrast, the solar-cell-based wearable device developed in this study overcomes the limitation. In an *in vitro* experiment, ES applied to various types of cells associated with angiogenesis significantly enhanced cell migration and secretion of angiogenic paracrine factors. To evaluate the therapeutic efficacy of the device *in vivo*, the electrode of the solar cell device was implanted into the

ischemic region of a mouse hindlimb, and the solar panel part of the device was attached to the back of mouse for exposure to light. The device successfully converted light energy into electrical energy and generated ES. ES induced cell migration and promoted the secretion of angiogenic paracrine factors. Furthermore, use of the solar cell device led to significant increase in the number of capillaries and arterioles at the ischemic region, and prevented muscle necrosis and loss of the ischemic limb.

Secondly, the chapter 4 investigated whether the IDM can enhance transplanted cell grafting and therapeutic efficacy. For fabrication of IDM, we applied lattice roller to confluently cultured ADSC and obtained uniform, well-structured decellularized matrix. Conventional method for acquisition of ECM includes proteolytic enzyme treatment such as pepsin, IDM fabrication in this study does not include protein decomposition step. Therefore, the IDM used in this study can be an ECM with a composition similar to the environment in which the cells are attached. In an *in vitro* experiment, IDM and ADSC complex (Cell-IDM) enhanced cell viability and upregulation of angiogenic paracrine factors. To evaluate the therapeutic efficacy *in vivo*, Cell-IDM was implanted into the ischemic region of a mouse hindlimb. Transplantation of Cell-IDM induced

significant increase in the number of capillaries and arterioles at the ischemic region, and prevented muscle necrosis.

# Chapter 2.

# Experimental methods

## 2.1. Fabrication and characterization of organic photovoltaic cell

### 2.1.1. Fabrication of organic photovoltaic cell

Photovoltaic cells were fabricated on indium tin oxide (ITO)-coated glass. The electron transport layer (30 nm) consisted of zinc oxide (ZnO), which was spin-coated onto the glass substrate by a sol-gel process. A photoactive layer (40 nm) consisting of poly(3-hexylthiophene) (P3HT) and phenyl-C61-butyric acid methyl ester (PCBM), (P3HT:PCBM solution 1:1 w/w, 2 wt/vol % in m-xylene), was then spin-coated onto the ZnO-coated substrate. A PEDOT:PSS as hole transport layer (40 nm) was spin-coated onto the photoactive layer. The cells were thermally annealed at 150°C for 10 min in a glove box with a nitrogen atmosphere. Top electrodes (Ag, 100 nm) were deposited onto the PEDOT:PSS layer by thermal evaporation under $5 \times 10^{-6}$ torr. Three photovoltaic cells were patterned in one substrate by shadow mask. The area of each cell was 16 $mm^2$.

### 2.1.2 Construction of implantable electrodes

Implantable electrodes were prepared on polyimide film (PI; length: 100 mm, width: 2 mm, thickness: 150 μm). Metal electrodes (Ti/Au, 5 nm/100 nm) were thermally evaporated at gaps of 5 mm on the PI film under $5 \times 10^{-6}$ torr. The electrodes were connected with the cathode and anode of an organic photovoltaic cell.

### 2.1.3 Characterization of organic photovoltaic cells

The photovoltaic characteristics of the cell patch were assessed using a Keithley 2400 source measurement device under white LED light (DI-LED-6W, SFS Lights, China) in air.

## 2.2. Fabrication and characterization of injectable decellularized matrix

### 2.2.1 Fabrication of injectable decellularized matrix (IDM)

hADCS incubated for 2 weeks in a 150-mm dish in DMEM medium. Then cultured cells were washed with phosphate buffered saline (PBS) once and added 10 ml of PBS. Under the PBS solution, cell cultures were cut in regular intervals using an ez passage lattice roller (Invitrogen). The lattice roller was drew in one direction and repeated after the dish turned 90 degrees to make lattice. Then cell culture was decellularized by using decellularization buffer (0.5% Triton X-100, 20mM $NH_4OH$ in PBS) from the method of previous report.[43] At this time, ECM sticks to the surface of the dish, then carefully scratched off using a cell scraper. Then collected by centrifugation at 2000g for 20 minutes. After that, washed twice with PBS to remove the decellurization buffer and treated the 100unit/ml DNase (Worthington bio) overnight.

### 2.2.2 IDM characterization

For the IDM characterization, cultured cell, decellularized ECM, and IDM were immunostained with anti-fibronectin antibody (Abcam). For the cell attachment assay, trypsinized cells were stained with PKH-26 staining kit (Invitrogen).

### 2.2.3 DNA content assay

Cultured cell, decellularized matrix, and IDM samples were obtained confluently cultured $1x10^6$ cells. Total DNAs were obtained with DNA extraction kit (Bioneer). DNA concentration was measured with nanodrop 2000 (Thermo Fisher Scientific). Then amount of DNA in $1x10^6$ ADSCs was calculated.

## 2.3. *In vitro* assays

### 2.3.1. Cell isolation and culture

*Endothelial progenitor cells.* Bone marrow (BM) cells collected from tibias and femurs of C57BL6/J mice aged 7weeks. BM cells were then plated on cell culture dishes coated with 1% gelatin (Sigma, St. Louis, MO, USA) at a density of $10^6$ cells/$mm^2$ and cultured in the EGM-2 BulletKit system (Lonza, Walkersville, MD, USA). After 5 days, non-adherent cells were discarded, and fresh culture medium was added. The medium was changed daily and the attached cells were used as the EPC-rich population for the following in vitro studies.

*Endothelial cells.* Mouse endothelial cells were isolated by an immunobead protocol from skeletal muscles of C57BL6/J mice aged 7weeks. After digestion of mouse skeletal muscle tissue using skeletal muscle dissociation kit (Miltenyi Biotec, Bergisch Gladbach, Germany), $CD31^+$ cells were separated using magnetic-activated cell sorting (MACS) (CD31+ Microbead Kit; Miltenyi Biotec, Bergisch Gladbach, Germany) according to the manufacturer's instructions and cultured in the EGM-2 BulletKit system (Lonza, Walkersville, MD, USA).

*Mouse mesenchymal stem cells.* Adipose tissue was obtained from

C57BL6/J mice. Adipose tissue was excised from the epiploon, cut into small pieces, digested in collagenase and filtered. Cells were cultured with Dulbecco's modified Eagle's medium (DMEM) supplemented with 10% fetal bovine serum (FBS) and antibiotics.

*Myoblasts.* Mouse myoblast cells were enzymatically dissociated from limb muscle tissue of C57BL6/J mice. Muscle tissue was digested using skeletal muscle dissociation kit (Miltenyi Biotec, Bergisch Gladbach, Germany). Cells obtained were maintained with DMEM supplemented with 10% FBS and antibiotics in a 5% $CO_2$ incubator at 37°C.

*Human mesenchymal stem cells.* Human mesenchymal stem cells were commercially purchased (Lonza, Walkersville, MD, USA). Cells were maintained with DMEM supplemented with 10% FBS and antibiotics in a 5% $CO_2$ incubator at 37°C.

*Human adipose derived mesenchymal stem cells.* Human mesenchymal stem cells were commercially purchased (Lonza, Walkersville, MD, USA). Cells were maintained with DMEM supplemented with 10% FBS and antibiotics in a 5% $CO_2$ incubator at 37°C.

The primarily-derived myoblasts, MSCs and EPCs phenotype were

examined with FACS. The primarily-derived mMSCs were CD105 positive and Sca-1 positive[44-46]. mEPCs were CD34 negative, c-kit negative, Flk-1 positive and VE-cadherin negative[47-48]. mMyoblasts were integrin α7 negative[49].

### 2.3.2. *In vitro* cell culture for electrical stimulation

*In vitro* cell culture chambers were constructed as previously reported[17]. Briefly, a teflon block and teflon lid were used as a mold for making a chamber. A glass slide was used as a surface for cell attachment. A rubber spacer was used to seal the chamber and prevent leakage of cell medium. Silicon tubes (15 cm long, 1.5 mm inner diameter) filled with 2% wt/vol agarose in PBS were used as salt bridges. After the cell culture chamber was constructed, the salt bridges were immersed in saline reservoirs connected to a power generator by Ag/AgCl electrodes, which were used to avoid electrolysis of the medium. The cell seeding density was 1000 cells/$mm^2$.

### 2.3.3. Scratching wound-healing assay

For the scratch migration assays, cells were seeded in slides and grown until confluence. A linear gap was created by scratching the cells of the slides using a sterile yellow tip. The cells were washed with each medium in order to remove the detached cells, and then electrically stimulated for 6 hours at 200mV/mm. Cell migration activity was observed under a microscope equipped with a 40x objective lens and expressed as the relative healing area : [(original scratch area - new scratch area)/original scratch area] ×100%.

### 2.3.4 Enzyme-linked immunosorbent assay

Cell culture supernatants were collected after 24 hours of electric stimulation and the concentrations of cytokine were measured by enzyme-linked immunosorbent assay kits for mouse SDF-1α, VEGF, FGF, HGF (R&D systems, Minneapolis, MN, USA).

### 2.3.5. Apoptosis assay

Apoptosis in each cells was measured after 24hr of electric stimulation by using a FITC Annexin V apoptosis detection kit (BD Pharmingen) according to the manufacturer's instructions. After staining, the % of viable, apoptotic and necrotic cells was quantified by flow cytometry (BD accuri C6).

### 2.3.6. Cell cycle analysis

For cell cycle analysis, Cells were collected after 24hr of electric stimulation and then washed with PBS, fixed in cold 70% ethanol at 4°C for 1hr, and incubated in 0.2mg/ml RNase A (Sigma-Aldrich, St. Louis, MO, USA) for 1hr at 37°C. Prior to analysis, cells were stained with 10μg/ml propidium iodide (PI; Sigma-Aldrich). Distribution of the cell cycle phase was determined with flow cytometry (BD FACS Canto 2). Data for cell cycle distributions were analyzed using BD FACSDiva software (BD Biosciences, Bedford, MA).

### 2.3.7. Surface marker expression analysis

Cells were subjected to flow cytometry analysis using the following: the labeled endothelial progenitor cell (EPC) markers CD34 (BD Pharmingen, San Jose, CA, USA), c-Kit (BD Pharmingen), Flk-1 (BD Pharmingen, San Jose, CA, USA), VE-cadherin (BD Pharmingen), and mesenchymal stem cell (MSC) markers CD90 (BioLegend, San Diego, CA, USA), CD105 (BD Pharmingen), Sca-1 (Thermo Fisher Scientific, Waltham, MA, USA), and skeletal muscle markers Integrin α1 (BioLegend), Integrin α7 (Miltenyi Biotec, Bergisch Gladbach, Germany).

### 2.3.8 Cell viability assay

The live and dead cells on non-coated graphene or VN-coated graphene were detected with fluorescein diacetate (FDA, Sigma–Aldrich, St. Louis, MO, USA) and ethidium bromide (EB, Sigma) at day 2. The dead cells were stained orange due to the nuclear permeability of EB. The viable cells, which are capable of converting the non-fluorescent FDA into fluorescein, were stained green.

### 2.3.9. *in vitro* hypoxic condition cell assay

To generate hypoxic culture conditions for the growth of hADSCs, culture dishes with hADSC monolayers or spinner flasks with hADSC spheroids were placed in hypoxic incubator (MCO-18M, Sanyo, Japan) containing 1% oxygen and 5% CO2 at 37 ℃ for 3 days.

### 2.3.10. IDM cell attachment assay

To calculate IDM attached cell percentage, IDMs were stained green with coumarine (100ug/ml). And the cells were stained red with DiI (Sigma). After mixing of IDMs and cells 0min, 10min, 30min, and 60min samples were examined under a fluorescence microscope.

## 2.4. *In vivo* assays

### 2.4.1. Modeling of hindlimb ischemia

Commercially available athymic mice (female, six-week-old, 20–25 g) were purchased from the local company (Orient, Seoul, Korea). After anesthesia (ketamine (100 μg/g) and xylazine (10 μg/g)), the femoral artery and its branches of the mice were ligated with 6-0 black silk sutures (Ailee, Busan, Korea). Then the external iliac artery and the upstream arteries were ligated. After that the femoral artery was excised from its proximal origin, as previously described[50-52].

All experimental procedures and animal treatments were agreed by the Institutional Animal Care and Use Committee of Seoul National University (No. SNU-160303-6).

### 2.4.2. Treatment of mouse hindlimb ischemia for solar cell implant

Instantly after hindlimb ischemia modeling, the mice were divided into four groups (n = 12 per group), like this: no treatment, electrode only (mice implanted with solar cell electrode without photovoltaic cell), human mesenchymal stem cell (hMSC) injection (MSC group), and solar-cell-induced ES (Solar cell). Negative control group was mice with arterial dissection only (no treatment group). The MSC group received injection of hMSC suspended in PBS (200 μl, $1 \times 10^6$ cells) into the medial thigh of the gracilis muscle on day 0. The MSC dose ($1 \times 10^6$ cells per mouse) was known to be optimal, based on previous studies[30, 53-54]. Mice in the solar cell group were implanted with the solar cell device, which consisted of implantable electrodes connected to the photovoltaic cell. The electrodes were implanted subcutaneously in medial thigh region. In all experimental group, the light source was set to 12 hour on and 12 hour off per day for 2 weeks.

### 2.4.3. Treatment of mouse hindlimb ischemia for Cell-IDM

Instantly after hindlimb ischemia modeling, the mice were divided into three groups (n = 12 per group), as follows : Sham, Cell, and Cell-IDM. Negative control group was mice with arterial dissection only (Sham group). The Cell group received injection of hADSC suspended in PBS (100 μl, $1 \times 10^6$ cells) into the medial thigh of the gracilis muscle on day 0. The MSC dose ($1 \times 10^6$ cells per mouse) was known to be optimal, based on previous studies[30, 53-54]. Mice in the Cell-IDM group group received injection of IDM mixed hADSC suspension in PBS (100 μl, 4mg of IDM and $1 \times 10^6$ cells).

### 2.4.4. Laser Doppler imaging analysis

Laser Doppler imaging (laser Doppler perfusion imager; Moor Instruments, Devon, UK) was performed for serial noninvasive physiological evaluations of neovascularization. Mice were monitored by serial scanning of the surface blood flow in hindlimbs on days 0, 7, 14, 21, and 28 after hindlimb ischemia treatment. Color-coded digital images were analyzed to quantify blood flow in the region from the knee joint to the toe, and the mean perfusion values were subsequently calculated.

### 2.4.5. Immunohistochemistry

At day 28 after hindlimb ischemia treatment, limb muscles were obtained from sacrificed mice. Then samples were embedded in optimal cutting temperature compound (Sakura Finetek, Torrance, CA). After sample freezing step, the samples were cut into 10-μm sections under −23°C. The ischemic region sections were subjected to immunofluorescent staining to quantify microvessels by anti-smooth muscle α-actin (SM α-actin) antibodies (Abcam, Cambridge, UK) and anti-CD31 antibodies (Santa Cruz Biotechnology, Santa Cruz, CA). Fluorescein isothiocyanate–conjugated secondary antibodies (Jackson ImmunoResearch Laboratories, West Grove, PA) were used to visualize the signals. The sections were counterstained with 4',6-diamidino-2-phenylindole (DAPI) and examined under a fluorescence microscope (Nikon TE2000, Tokyo, Japan). The total number of fluorescent vessels in the thigh muscle region from the hindlimb was determined.

### 2.4.6. Histological examination

At 28 days after treatment, the thigh muscles of the ischemic limbs were collected. Ischemic limb muscle specimens were fixed in formaldehyde, dehydrated in a graded ethanol series, and embedded in paraffin. Paraffin-embedded specimens were sliced into 4-μm thick sections and stained with hematoxylin and eosin (H&E) to assess muscle degeneration and tissue inflammation. Masson's trichrome collagen staining was also performed to assess tissue fibrosis in the ischemic regions.

### 2.4.7. Western blot analysis

The mouse limb muscle samples and the cell samples were lysed with a electric homogenizer in cell lysis buffer (Cell Signaling Technology, Danvers, MA). Protein concentrations were determined by a bicinchoninic acid protein assay (Pierce Biotechnology, Rockford, IL). Equal protein from each sample were mixed with sample buffer, loaded, and subjected to sodium dodecyl sulfate–polyacrylamide gel electrophoresis (SDS-PAGE) using a 10% (v/v) resolving gel. Proteins separated by SDS-PAGE were transferred to an Immobilon-P membrane (Millipore, Billerica, MA) and then probed with antibodies against smooth muscle α-actin (SM α-actin), CD31, CD34, HGF, FGF2, VEGF, and SDF-1α (CD31 and CD34 from Santa Cruz Biotechnology, the others from Abcam, Cambridge, UK) for 1 hour at room temperature. After then the membranes were submerged with horse radish peroxidase-conjugated secondary antibody (Santa Cruz Biotechnology, Dallace, TX) for 1 hour at room temperature. The blots were developed using an Gel logic imaging system (Carestream Health, Rochester, NY). Bands were imaged and quantified through Image J program.

### 2.4.8. Transplantation of PKH26-labeled hMSCs

To estimate the effect of ES on MSC homing, hMSCs were labeled by PKH26 (Sigma, St. Louis, MO) and injected into mice intravenously ($1 \times 10^6$ cells in 100 μL of PBS per mice) after the hindlimb ischemia modeling. 5 days after the treatments (electrode implantation, MSC injection, or ES treatment), the animals were sacrificed. After frozen sectioning, PKH26-positive cells in the ischemic region of the hindlimb were directly counted by microscopy examination to quantify the migration of the MSCs in the ischemic limb region.

### 2.4.9. Live imaging

To evaluate the cell grafting and retention after the transplantation, hADSCs (Lonza, Basel, Swiss) were labeled by VivoTrack 680 (PerkinElmer) and injected into ischemic muscle ($1 \times 10^6$ cells in 100µL of PBS per mice). Luminescence intensity was monitored and quantified during 28 days using IVIS spectrum live imaging system (PerkinElmer).

## 2.5. Statistical analysis

Quantitative data were expressed as mean ± SD. OriginPro 8 software (OriginLab, Northampton, MA) was used to perform the one-way analysis of variance test. Hindlimb salvage was evaluated with SAS/STAT software (SAS Institute, Cary, NC). Statistically significant means that *P* values less than 0.05.

# Chapter 3.

# Therapeutic angiogenesis *via* solar cell facilitated electrical stimulation

## 3.1. Introduction

Cell-based therapy has been proposed as a treatment for ischemic diseases[55]. Implantation of a number of different cell types, including mesenchymal stem cells (MSCs)[56-60], embryonic stem cells[61-63], and induced pluripotent stem cells[64-66], has resulted in successful angiogenesis in ischemic disorders. Two mechanisms, namely differentiation of implanted stem cells into vascular cells and paracrine factor expression by implanted stem cells, are primarily responsible for tissue regeneration in ischemic diseases[67]. Increasing evidence suggests that secretion of therapeutic paracrine molecules from the implanted cells plays an integral role in tissue regeneration in ischemic diseases[68-69]. However, poor survival and engraftment of cells implanted into ischemic tissues limit their therapeutic efficacy[70].

Electrical stimulation (ES) has been suggested to be a promising approach for regenerating tissue, which can overcome the limitations of conventional stem cell therapy[15-18]. Endogenous electrical field (EF) is generated in the vasculature when angiogenesis occurs, which is generated by active ion transport across endothelium[19]. A previous study demonstrated that ES of the ischemic region resulted in strong upregulation of the expression of vascular endothelial growth factor (VEGF) by skeletal

muscle cells, and significantly enhanced angiogenesis for tissue regeneration[16]. Another study demonstrated that ES promoted the reorientation and migration of endothelial cells *in vitro*, which was mediated through PI3K-Akt/Rho-ROCK signaling pathways and reorganization of the actin cytoskeleton[20]. When skin is injured, a transepithelial potential difference develops at the layer of skin tissue, and the potential difference induces an electrical field at the wound, which persists until re-epithelialization is complete[21]. The endogenous EF induces migration of epithelial cells toward the wound in order to regenerate tissue, and wound healing is compromised when the endogenous EF is inhibited[22].

Although EF in wound healing has recently been studied[23], the role of ES or EF in therapeutic angiogenesis and subsequent tissue repair for ischemic diseases has not been clearly elucidated. ES was previously shown to direct the behavior of cells involved in the healing wounds[22]. Hence, we hypothesized that ES may modulate the behavior of the types of cells specifically involved in angiogenesis, which include MSCs, myoblasts, endothelial progenitor cells (EPCs), and endothelial cells (ECs). These cells all contribute to the formation of microvessels in the ischemic region. To elucidate the therapeutic effect of ES on angiogenesis, we developed a solar-cell-based ES-generating device and tested the

therapeutic effect of ES on various types of angiogenic cells *in vitro*, and also investigated the effect of ES on *in vivo* angiogenesis in an animal model of ischemic disease.

In this study, we investigated whether the solar-cell-based device, which converts light energy to electrical energy, can generate an electrical stimulus that would control cell behavior and stimulate therapeutic angiogenesis in a mouse ischemic hindlimb. For easy utilization of the device *in vivo*, we designed a solar cell circuit that consisted of an implantable electrode and a solar panel that adhered to the skin. Conventional clinical ES usually involves a large electrical device, which may require patient hospitalization. By contrast, the solar-cell-based wearable device developed in this study overcomes the limitation. In an *in vitro* experiment, ES applied to various types of cells associated with angiogenesis significantly enhanced cell migration and secretion of angiogenic paracrine factors. To evaluate the therapeutic efficacy of the device *in vivo*, the electrode of the solar cell device was implanted into the ischemic region of a mouse hindlimb, and the solar panel part of the device was attached to the back of mouse for exposure to light. The device successfully converted light energy into electrical energy and generated ES. ES induced cell migration and promoted the secretion of angiogenic

paracrine factors. Furthermore, use of the solar cell device led to significant increase in the number of capillaries and arterioles at the ischemic region, and prevented muscle necrosis and loss of the ischemic limb.

## 3.2. Results

### 3.2.1. *In vitro* cell migration and angiogenic paracrine factor secretion by various cell types induced by ES

To investigate cell migration *in vitro* in ES, mouse mesenchymal stem cells (mMSC), mouse myoblasts (mMyoblast), mouse endothelial progenitor cells (mEPC), and mouse endothelial cells (mEC) were cultured with or without ES. The cell migration was promoted significantly with ES, regardless of the cell type (Figure 3.1b, d, f, and h). The data suggest that stem cell homing and angiogenic cell migration, which are critical for angiogenesis, can be improved by ES.

In ischemic tissue, the core mechanism for angiogenesis is expression of angiogenic factors by stem cells. Thus, to determine whether ES leads to enhanced *in vitro* expression of angiogenic factors, we measured the quantities of the angiogenic factors expressed by various cells. The levels of angiogenic factors including HGF, FGF2, VEGF, and SDF-1α were significantly higher in the ES-treated cells than in the control cells (without ES treatment) (Figure 3.1c, e, g, and i). The higher levels of SDF-1α and VEGF may be attributed to the enhanced cell migration.

We analyzed cell apootosis through annexin V / PI staining. As shown in

the Figure 3.2, the electrical stimulation group showed increased live cell percentage in mMSC, mEPC and mMyoblast cell type. In mEC cell type, the percentage of apoptotic cells increased but the percentage of live cells was not affected by the electrical stimulation. These results indicate that electrical stimulation does not adversely affect cell death. In addition, we analyzed cell cycle through PI analysis. As shown in the figure 3.3, the electric stimulation did not affect on cell cycle (Figure 3.2 and 3.3).

a

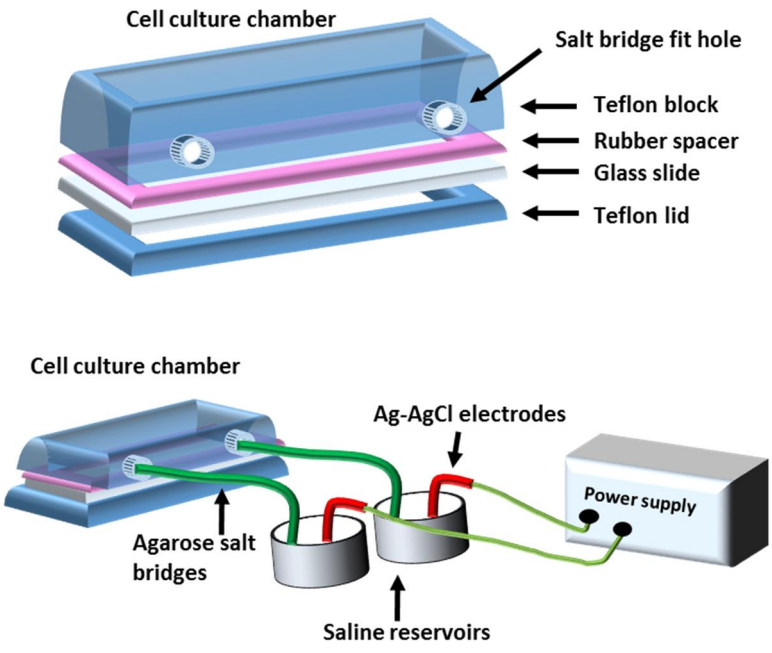
Cell culture chamber
Salt bridge fit hole
Teflon block
Rubber spacer
Glass slide
Teflon lid
Cell culture chamber
Ag-AgCl electrodes
Power supply
Agarose salt bridges
Saline reservoirs

**Figure 3.1. a**

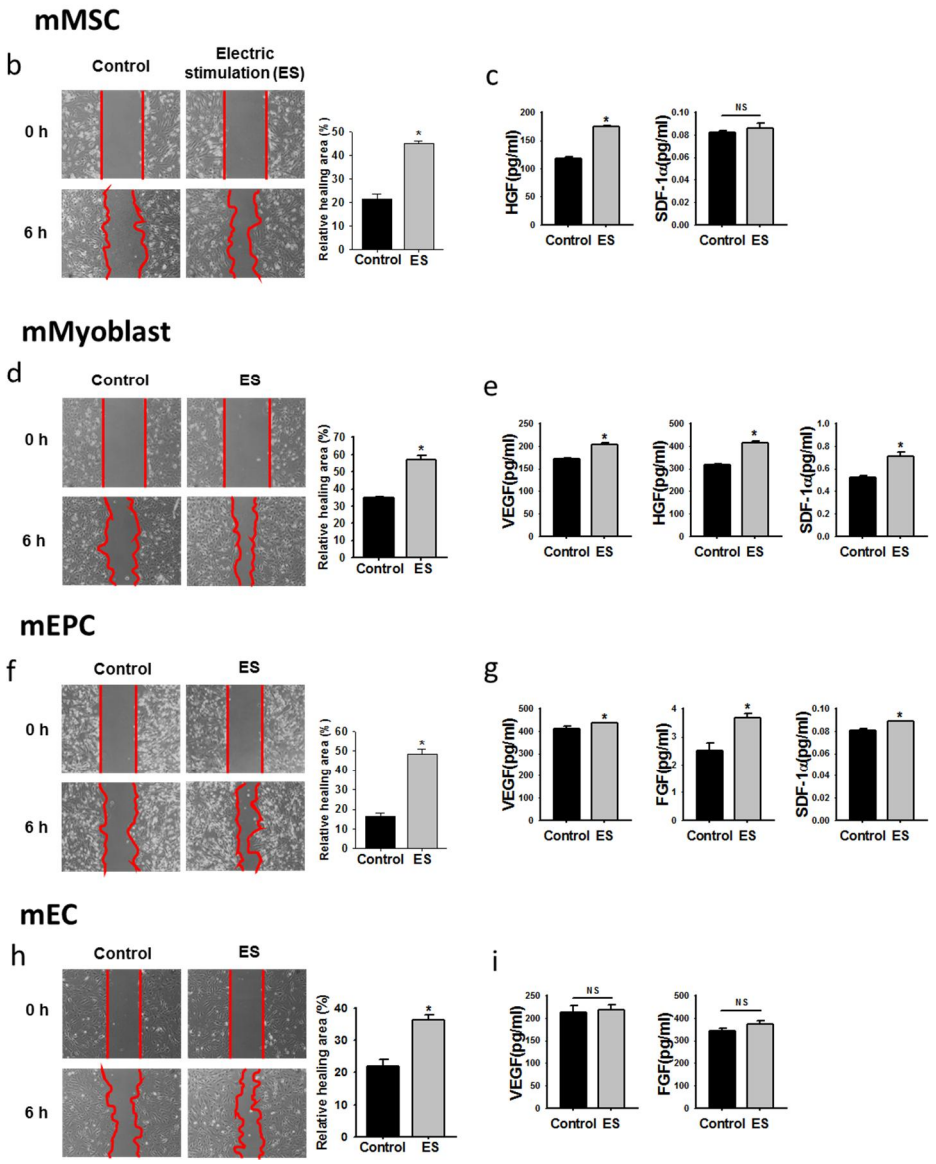


**Figure 3.1.** Enhanced cell migration and angiogenic paracrine factor secretion as a result of ES generated from a solar cell device. (a) Schematic figure of cell culture chamber for ES. ES improved cell migration of (b) mMSC, (d) m-myoblasts, (f) mEPCs, and (h) mECs, as evaluated by the cell migration assay. ES also improved angiogenic paracrine factor

secretion by (c) mMSC, (e) m-myoblasts, (g) mEPCs, and (i) mECs, as evaluated by ELISA. Cells cultured without ES served as the controls. *$P < 0.05$ compared with the ES group. NS denotes “not significant”.

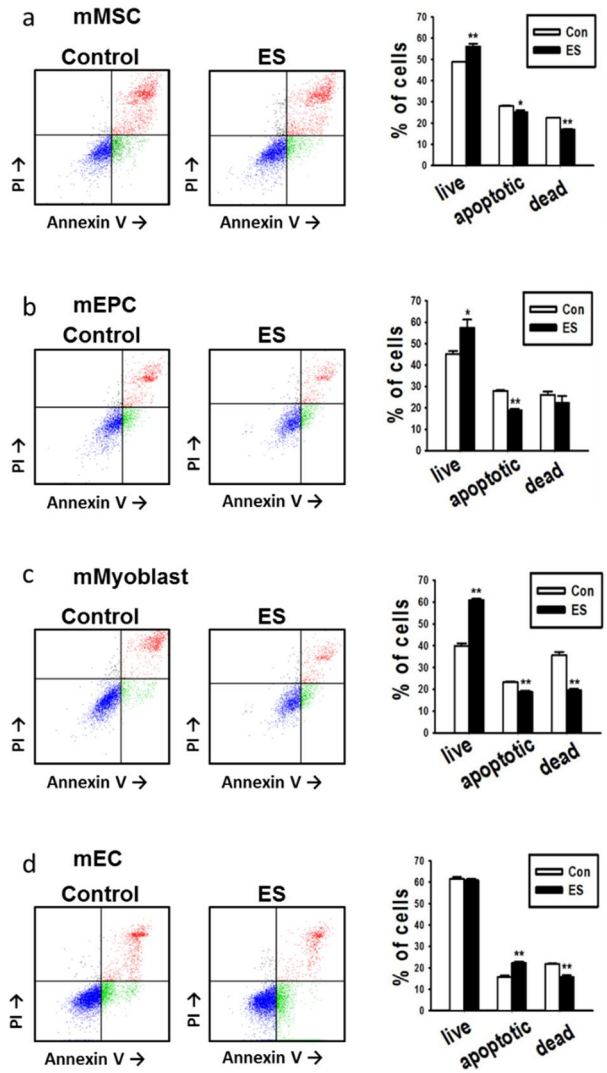


**Figure 3.2.** Evaluation of cell apoptosis using annexin V/PI staining. Cells were treated with 24hr of electrical stimulation (ES). Dot plot profile and the percentage of apoptotic and dead cells were analyzed by FACS. (a) mMSC, (b) m-myoblasts, (c) mEPCs, and (d) mECs. Cells cultured without ES served as the controls (Con = control). *$P < 0.05$ compared with the ES group. **$P < 0.01$ compared with the ES group. PI = propidium

iodide.

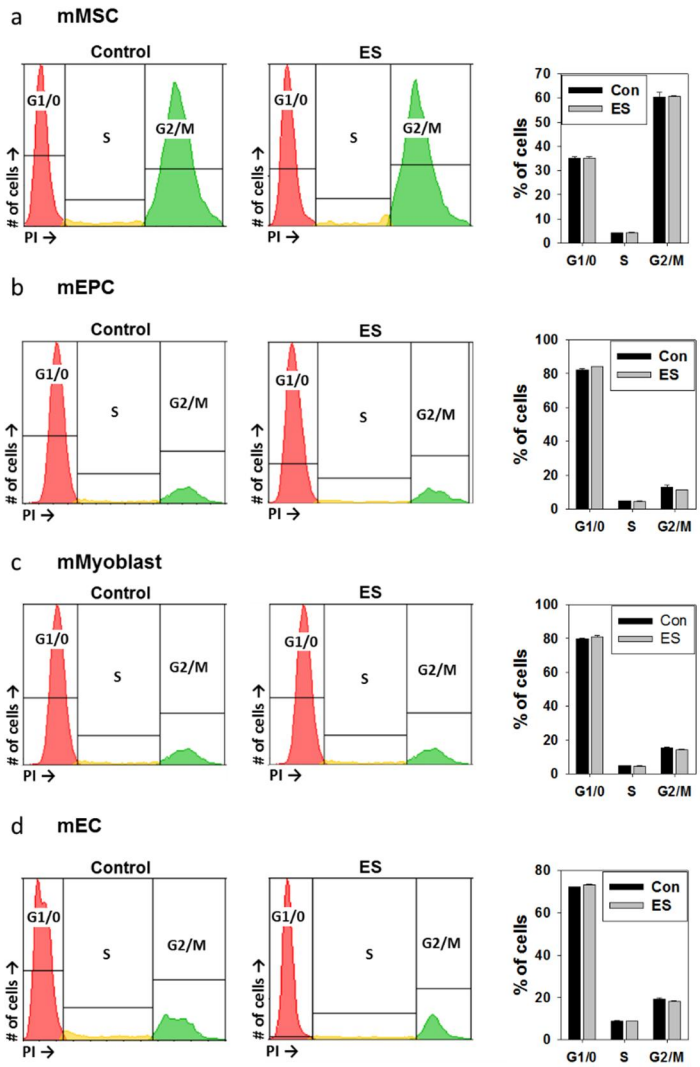


**Figure 3.3.** Evaluation of cell cycle using PI staining. Cells were treated with 24hr of electrical stimulation (ES). After fixation, the cells were stained with PI and then analyzed using a flow cytometer. (a) mMSC, (b) m-myoblasts, (c) mEPCs, and (d) mECs. Cells cultured without ES served as the controls (Con = control). PI = propidium iodide.

### 3.2.2. Photovoltaic capacity of solar cell device

The electrodes of the devices were constructed of polyimide film coated with gold (Figure 3.4a). A solar cell was attached to the back of mouse, and the corresponding electrode was implanted into the ischemic region of the hindlimb (Figure 3.4b). To determine the photovoltaic capacity of the ES-generating device, the current and output voltage were measured under a 6W white LED. For the *in vivo* experiment, the maximum angle between the light source and the photovoltaic solar cell was fixed at 34.7˚ (Figure 3.4c). Figure 3.4d shows current-versus-voltage (I-V) curves of the photovoltaic cell at various angles of light. Although the voltage output decreased with increasing angle of light because of reduced light density, the minimum voltage output was higher than 1V (Figure 3.4e). In addition, the applied voltage was calculated for the resistance of hindlimb muscle (≈ 100 kΩ). The applied voltage was similar to the voltage output of the solar cell circuit. The intensity of the electrical stimulation used in this experiment (200mV/mm) is much smaller than the difference in membrane potential during muscle contraction[71]. During and after the electrical stimulation we did not observe abnormal muscle contraction and pathological abnormalities in the thigh muscle region. We next

investigated the immune response and histopathology of the electrode implantation and electrical stimulation. The skin incision group (Sham) was used as a control group. There was no significant difference between the three groups (i.e. Sham, Electrode only, and Solar cell) in the histological analysis. Staining for macrophages with anti-CD68 indicated that there was not many macrophages near the implanted electrodes. Therefore, the electrode caused no significant inflammatory response (Figure 3.5).

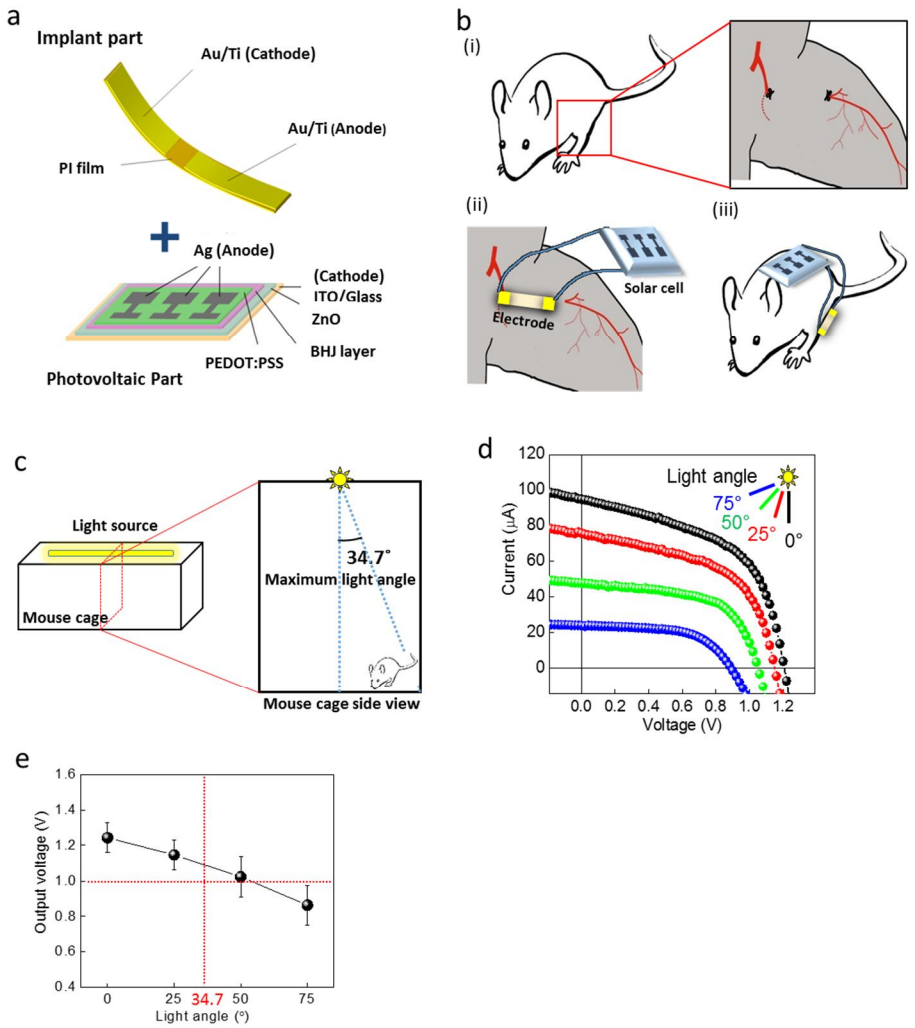


**Figure 3.4.** Schematic figure showing solar cell circuitry and *in vivo* experiment. (a) Solar cell designed for *in vivo* experiment. (b) Schematic figure for *in vivo* experiment using solar cells. After hindlimb ischemia modeling, the Au/Ti-coated polyimide (PI) film was implanted into the ischemic area and connected to the photovoltaic cell by wires. The photovoltaic cell was attached to the back of the mouse. (c) Schematic figure of light source attached to the roof of the mouse breeding cage. A

6W white LED was used as the light source. The maximum angle between the light source and the photovoltaic cell was fixed at 34.7˚. (d) Photovoltaic capacity of the solar cell according to changes in the angle of light. (e) Voltage output of the solar cell according to changes in the angle of light.

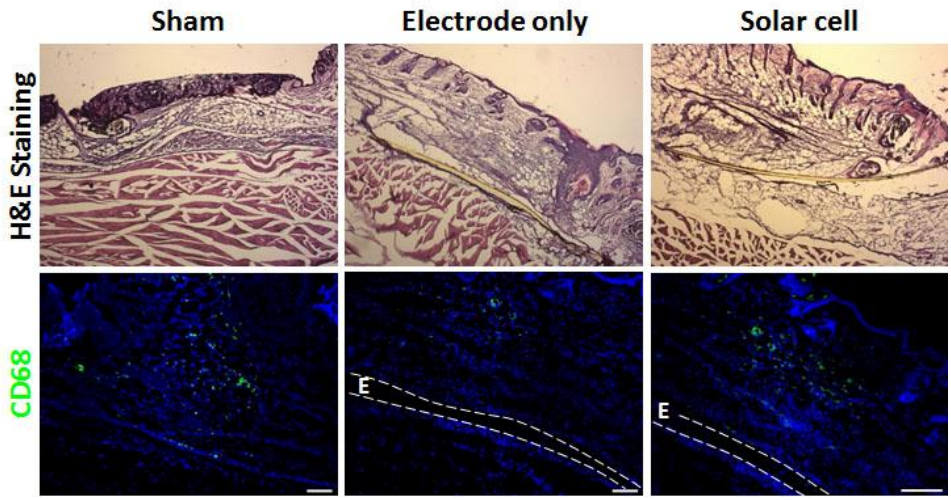


**Figure 3.5.** Histological evaluations of the electrode implantation region. Tissues in the implantation regions were stained with H&E and CD68 immunohistochemistry (green) at 3 days after implantation. Scale bars = 100 μm. Blue indicates nuclei stained with 4,6-diamidino-2-phenylindole (DAPI). E = electrode.

### 3.2.3. *In vivo* homing of MSCs

Angiogenic stem or progenitor cells recruitment is another important mechanism for angiogenesis in ischemic tissue. To determine whether ES stimulates MSC homing to the ischemic region, we evaluated hMSC homing at the ischemic region. The number of PKH26-positive cells in the solar cell group was significantly higher than that of PKH26-positive cells in the MSC injection group (Figure 3.6). This result can be explained by the enhanced level of SDF-1α in the ischemic region (Figure 3.7), which cause progenitor or stem cells recruitment. Taken together, these results indicate that ES can improve MSC recruitment and expression of angiogenic factors in the ischemic region.

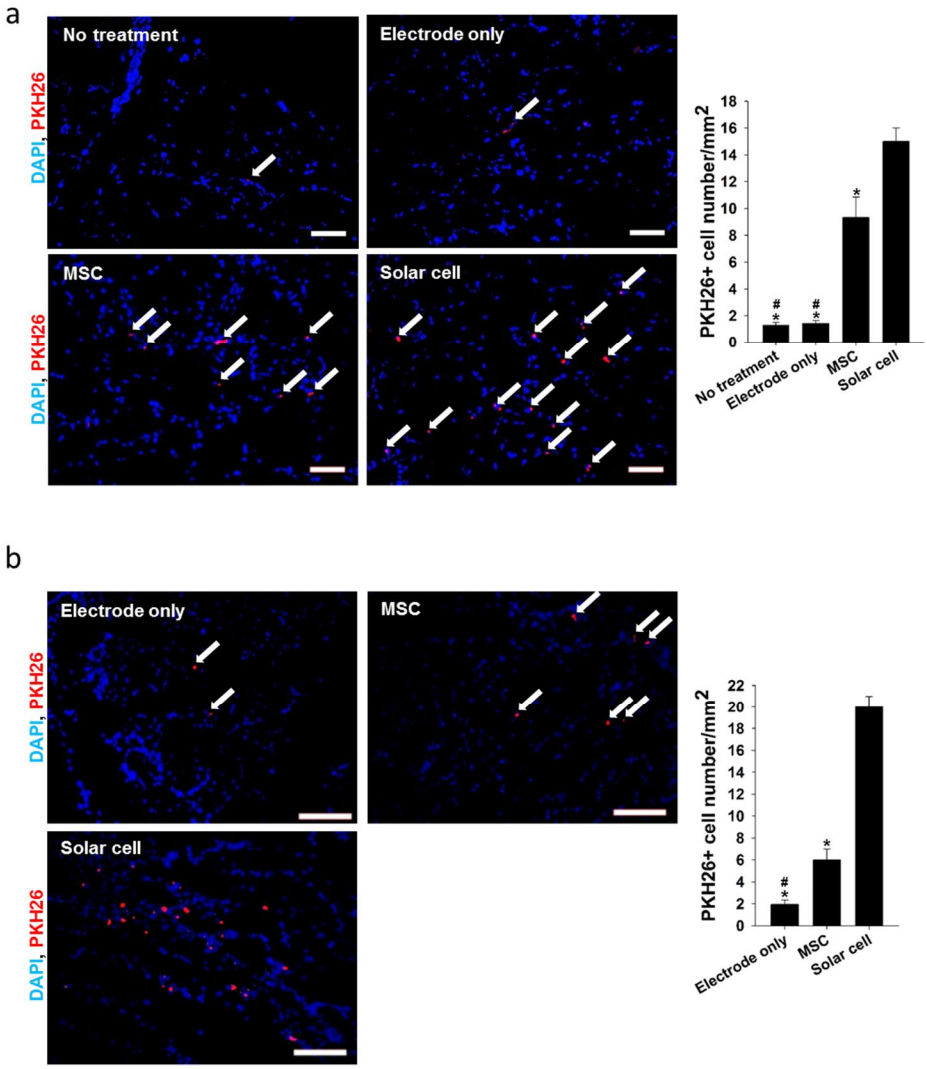


**Figure 3.6.** Enhanced MSC and EPC homing. (a) PKH26-labeled hMSCs (red) and (b) PKH26-labeled mEPCs (red) congregated in the ischemic tissue after intravenous injection of PKH26-labled hMSCs and PKH26-labled mEPCs. To evaluate the effect of ES on MSC and EPC homing, PKH26-labled hMSCs and mEPCs were injected. After sampling and frozen sectioning, PKH26-positive cell number in the limb tissues was

calculated (white arrows). DAPI (blue) indicates counter stained labled cells. Scale bars = 100 μm. *$P < 0.05$ compared with the solar cell group. #$P < 0.05$ compared with the MSC group, n = 10 per group.

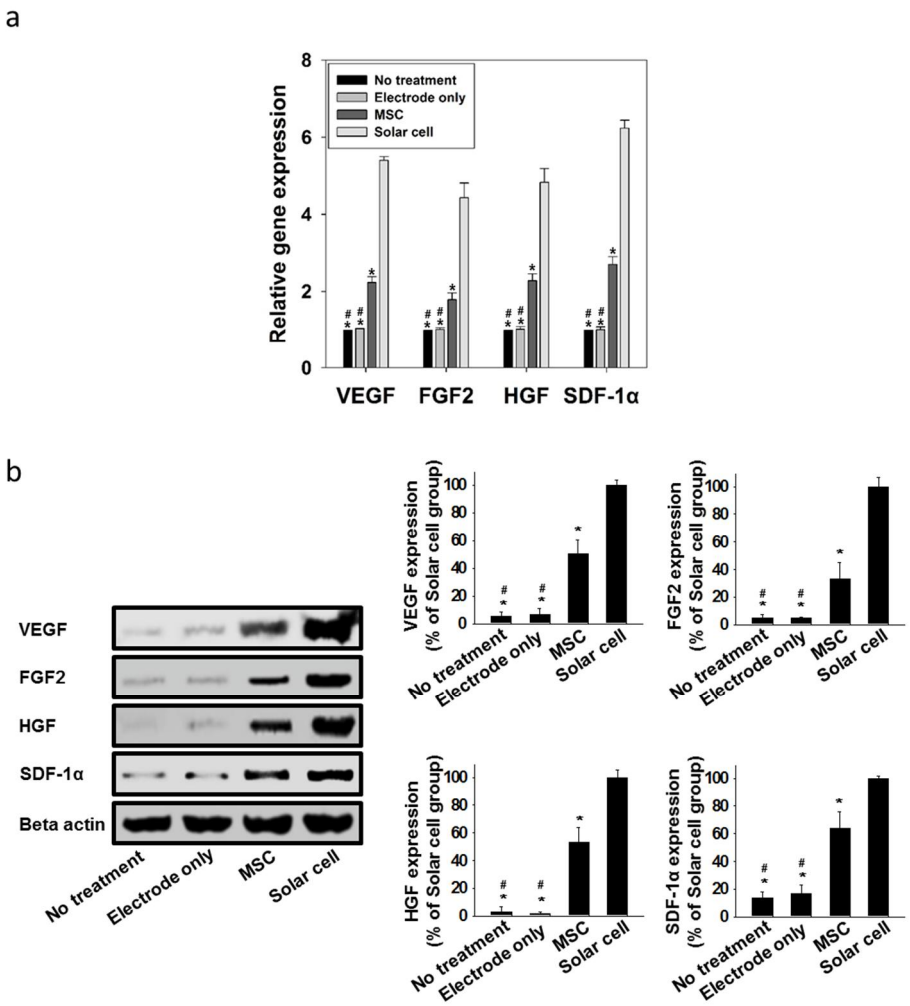


**Figure 3.7.** Enhanced angiogenic paracrine factor secretion induced by ES generated from the solar cell device. (a) Enhanced angiogenic paracrine factor expression in the ischemic hindlimb tissues associated with ES. Mouse VEGF, mouse FGF2, mouse HGF, and mouse SDF-1α mRNA expression was determined by q-PCR analysis. *$P < 0.05$ compared with the solar cell group. #$p < 0.05$ compared with the MSC group, n = 4. (b)

Enhanced angiogenic paracrine factor expression in the ischemic hindlimb tissues associated with ES. Mouse VEGF, mouse FGF2, mouse HGF, and mouse SDF-1α protein expression was determined by western blot analysis. To compare the angiogenic efficacy of the solar cell, MSCs that were known to be angiogenic were implanted (the MSC group). *$P < 0.05$ compared with the solar cell group. #$p < 0.05$ compared with the MSC group, n = 4.

### 3.2.4 Microvessel density in ischemic limbs

Immunofluorescent staining using antibodies against CD31 and SM α-actin was performed to evaluate microvessel density in the ischemic hindlimbs 28 days after treatment (Figure 3.8). SM α-actin- and CD31-positive microvessel density in the solar cell group was significantly increased compared to the other groups. Western blotting of the ischemic tissues showed that CD31, SM α-actin, and CD34 (MSC and EPC marker)[72] expression was significantly escalated in the solar cell group (Figure 3.9). The higher levels of MSC recruitment and angiogenic factors in the ischemic region are likely to cause more extensive angiogenesis in the solar cell group.

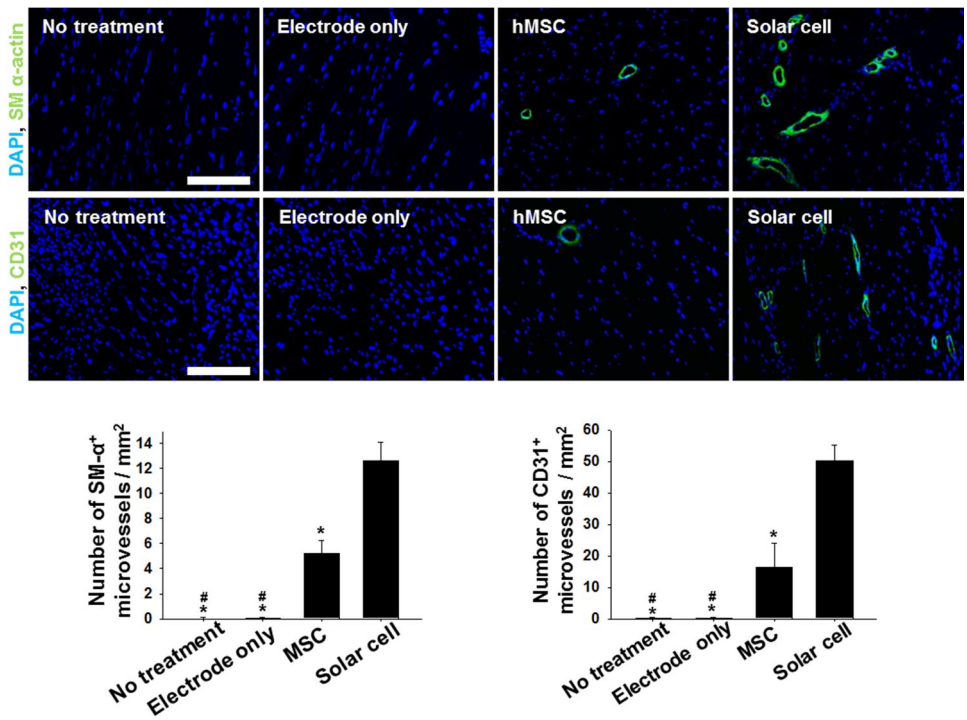


**Figure 3.8.** Enhanced microvessel formation in mouse hindlimb ischemic regions associated with ES generated from solar cells. Green indicates SM α-actin positive microvessels in upper part and CD31-positive microvessels in lower part at 28 days after treatment. Scale bars = 100 μm. Blue indicates nuclei stained with 4,6-diamidino-2-phenylindole (DAPI). **P* < 0.05 compared with the solar cell group. #*P* < 0.05 compared with the MSC group. n=12 per group.

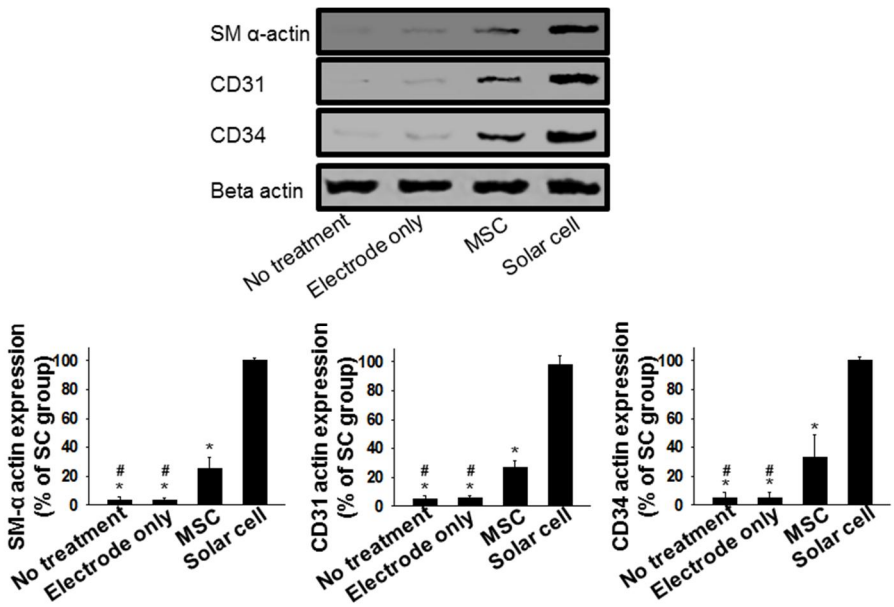


**Figure 3.9.** Increased secretion of angiogenic factor in the mouse hindlimb ischemic regions associated with ES generated from solar cells. SM-α-actin, CD31, and CD34 protein expression in the ischemic tissue of mouse hindlimbs, as determined by western blot analysis. **P* < 0.05 compared with the solar cell group. #*P* < 0.05 compared with the MSC group. n=4 per group.

### 3.2.5 Limb perfusion and limb salvage of the ischemic limb

Every 7 days after the hindlimb ischemia treatments, limb perfusion rate of ischemic limbs and limb salvage were monitored. More mice in the solar cell group had salvaged limbs than the other groups (Figure 3.10a and b). In the solar cell group, limb loss was decreased compared to any other group. Moreover, in the solar cell group the limb perfusion rate was significantly increased compared to that of other groups (Figure 3.10c). H&E and Masson's trichrome staining showed less tissue necrosis and fibrosis in the solar cell group than that of the other groups (Figure 3.10d).

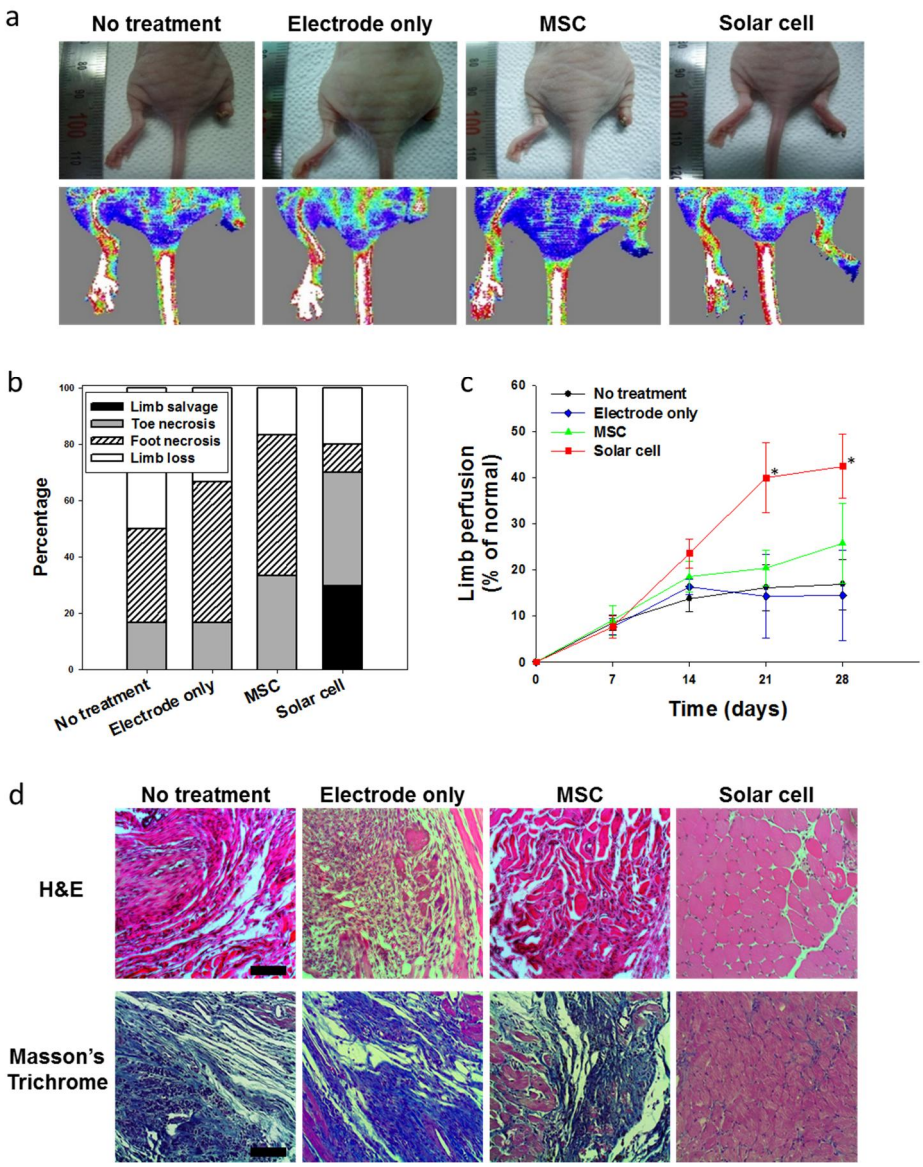


**Figure 3.10.** Improved limb salvage and blood flow with decreased fibrosis in the ischemic region of mouse hindlimbs associated with ES generated from solar cells. (a) Upper panel: representative photographs of ischemic limbs 28 days after treatment. Lower panel: laser Doppler images

presenting blood perfusion of ischemic limb 28 days after treatment. (b) Proportions of four status for each group (limb salvage, limb loss, toe necrosis, and foot necrosis) (n = 10 per group). (c) Monitored ischemic limb blood perfusion for 28 days (n = 10 per group). *$P < 0.05$ compared to either no treatment, electrode only, or MSC group. (d) Histological evaluations of the hindlimb ischemia region. Tissues in the ischemic regions were stained with H&E (upper panel) and Masson's trichrome staining (lower panel) at day 28 (Scale bars = 25 μm).

## 3.3. Discussions

ES has been widely used to induce neurogenic and cardiomyogenic regeneration[73-74]. Additionally, ES was shown to modulate the behavior of cells involved in angiogenesis[75], and to promote migration of and paracrine secretion by MSCs and ECs[76-77]. In agreement with the findings from previous studies, we found that ES greatly promoted migration of and angiogenic factor secretion by MSCs, myoblasts, EPCs, and ECs (Figure 3.1). Various mechanisms are involved in the increased migration of cells[18, 78-79]. Angiogenic paracrine factor secretion by cells was seen in studies showing that calcium channels and the calmodulin pathway served as the major transducers of the ES of cells[18, 80]. Additionally VEGF receptor signaling was shown to induce EPC migration associated with ES[78]. In addition to these signaling pathways, a number of other cellular signaling pathways that can affect the angiogenic paracrine secretion of various types of cells were previously described[81].

Several studies have demonstrated the promotion of tissue regeneration by exogenous ES[15-18, 21]. Although these studies introduced the idea of using ES for tissue regeneration, most ES-generating systems have required ES-generating extracorporeal devices and patient hospitalization.

To overcome limitations in the portability of ES-generating devices and promote patient-friendly therapeutics, we designed a wearable device that generates ES from light energy. Previous studies have demonstrated that 200mV/mm is the minimum voltage required for stimulating angiogenesis by mouse ECs and MSCs[21, 78, 80], and our device showed a minimum voltage output of 1V with the light angle at a maximum. Different voltage used for ES may induce different effects on the cells. A previous study has shown that cardiomyogenic differentiation is induced when an electrical stimulus of 1V/ mm is applied to embryonic stem cells[82]. Another study has shown that electrical stimulation of 100-170mV/mm induced differentiation of keratinocytes[83].

The use of solar cell-derived ES at the wound site significantly promoted angiogenesis compared with the injection of MSCs alone (Figures 3.8-3.10). Since the therapeutic mechanism (i.e., paracrine factor secretion and angiogenic cell homing) is similar to that of MSC therapy, MSC implantation was used as a control group to compare the therapeutic effect of the electric stimulation. Enhanced angiogenesis may be attributable to increased paracrine secretion at the site of ischemic tissue and the mobilization of bone marrow cells, including EPCs, toward the ischemic region. A previous study demonstrated that ES mediates MSC

homing[84]. Confirming the result of the previous study, our study found that solar-cell-derived ES induced significantly enhanced homing to the ischemic tissue of PKH26-labeled MSCs that had been injected 5 days after treatment (Figure 3.6) and increased the expression of angiogenic paracrine factors (Figure 3.7). Enhanced homing of MSCs to the ischemic site was in part facilitated by the higher expression of SDF-1a at the ischemic region (Figure 3.7). Increased angiogenic paracrine secretion by MSCs and skeletal muscle cells in association with ES have been previously reported[16, 85-86]. Not only MSCs enhance angiogenesis, but also EPCs play a pivotal role either directly or indirectly in vascular regeneration. They can repair damaged tissues through a direct process called angio/vasculogenesis by *in situ* incorporation and differentiation of the cells[87]. Besides they can contribute indirectly to vascular regeneration through the secretion of various pro-angiogenic factors[88]. EPCs have the ability to differentiate into endothelial lineage cells and promote neovessel formation in response to angiogenic cytokines and/or ischemic signals[89]. In briefly, ischemic signals upregulate VEGF or SDF-1, which is released to the circulation and stimulates recruitment of EPCs to the site of injury. The next step of EPC recruitment involves adhesion of the cells to ECs activated by cytokines and subsequent transmigration of the cells through

the EC monolayer. We examined how many EPCs are recruited to hindlimb ischemia region. As shown in Figure 3b, electrical stimulation induced recruitment of more EPCs compared with either the no electrical stimulation (Electrode only) group or the hMSC injection (MSC) group.

In this study, we fabricated an ES-generating solar cell device and demonstrated that the use of this device for a mouse model of ischemic hindlimb significantly enhanced therapeutic angiogenesis. The solar cell panel used in this study was fabricated with inflexible plastic for uniform light uptake, which led to stable energy generation. For the future use of our solar cell device for various types of diseases and parts of the body, the current system can be further developed to include a flexible attachable solar patch. Further studies of this device are needed. This study provided a disposable and easily usable and implantable ES-generating solar cell device that will not require hospitalization of patients needing treatment for angiogenic disease.

# Chapter 4.

# Injectable decellularized matrix for therapeutic angiogenesis

## 4.1. Introduction

Stem cell therapy has great potential for therapeutic angiogenesis to treat ischemic diseases. Endothelial progenitor cells derived from embryonic stem cells contribute to postnatal neovascularization by directly participating in blood vessel formation.[51] Mesenchymal stem cells (MSCs) derived from bone marrow and adipose tissues mainly induce angiogenesis through paracrine secretion of angiogenic growth factors.[90-91] Despite the potential, stem cells implanted to ischemic region have shown a low therapeutic efficacy because of their low survival rate, which is a large obstacle in clinical trials.[92] In ischemic region, implanted stem cells are immediately exposed to harsh conditions and prone to apoptosis.[93] One of the major aspects of implanted cell apoptosis is anoikis, which is cell apoptosis due to loss of cell adhesion to extracellular matrix (ECM).[93] *Ex vivo* cultured stem cells are harvested for implantation from culture plates through proteolytic enzyme (e.g., trypsin) treatment. Since the proteolytic enzyme treatment causes a loss in ECM from the harvested cells, cell adhesion signals are downregulated in harvested and subsequently implanted cells.[67] Indeed, within a few days after cell transplantation a high level of implanted cell death was observed in a number of animal

studies.[13-14] Moreover, clinical studies on the treatment of ischemic disease have shown that stem cell implantation had insignificant therapeutic efficiency due most likely to poor survival of the implanted cells.[92, 94-96]

To improve the engraftment of stem cells implanted to ischemic tissues, several strategies have been developed. The strategies include preconditioning of stem cells[29, 97], genetic modifications of stem cells[29, 98-99], combination of stem cell therapy with growth factors delivery[100], and use of tissue engineering scaffolds[101]. While preconditioned stem cells showed higher engraftment, the risk of cell damage and differentiation during the preconditioning procedure should be solved before clinical tials.[29] Genetic modification of stem cells have suffered from low transfection efficiency, mutagenic potential of target genes, and cytotoxicity.[102-103] Combination with growth factor delivery can enhance the stem cell survival, but local and controlled release system must be developed to avoid potential side effects and preserve the growth factor activity *in vivo*.[37]

In tissue engineering, synthetic polymer scaffolds or biologically derived ECMs can be used as a cell carrier for implantation. These matrices provide implanted cells with cell-adhesion cue for cell survival following

implantation.[38-39, 104] Several studies reported that cell implantation with a hydrogel containing ECM components enhanced therapeutic efficacy in animal models of myocardial infarction, limb ischemia, and bone fracture.[105-107] Hence, here we tested a hypothesis that injection of therapeutic cells adherent to injectable decellularized matrix (IDM) to ischemic sites may improve grafting of the cells end enhance angiogenic efficacy of the cells.

For fabrication of IDM, we applied a roller cutter to confluently cultured human adipose-derived stem cells (hADSCs) and treated the cell layer with decellularization solution to obtain approximately 80 μm-sized IDM (Figure 4.1). hADSCs were allowed to adhere to IDM. It was investigated whether the constructs of hADSCs and IDM (cell-IDM) enhanced the cell viability and upregulated angiogenic factor expression *in vitro* under either cell-adhesion suppression condition or hypoxic condition, which simulates microenvironments of ischemic tissues. Next, the cell-IDM was implanted into the ischemic region of mouse hindlimbs to investigate whether the implantaion of cell-IDM improves the angiogenic efficacy of the hADSCs by improving the engraftment of the implanted hADSCs (Figure 4.1).

## 4.2. Results

### 4.2.1. Fabrication of Cell-IDM complex

IDM as a hADSC implantation vehicle was manufactured from hADSC culture (Figure 4.1) because hADSCs would interact best with ECM produced by the same cells (i.e., hADSC). The amount of IDM produced from $10^6$ hADSC culture was approximately 2 mg. To characterize IDM, immunostaining for fibronectin and quantification of DNA content were performed. Immunostaining showed that fibronectin, a major ECM for cell adhesion, sufficiently remained after the decellularization process (Figure 4.2a). The DNA content quantification of cultured hADSCs, decellularized ECM, and DNase-treated decellularized ECM showed that IDM produced by decellularization and DNase treatment had no DNA (Figure 4.2b). The size of rectangular shaped IDM was approximately 80 μm. Several hADSCs were attached to a piece of IDM after incubation for 30 min (Figure 4.2c).

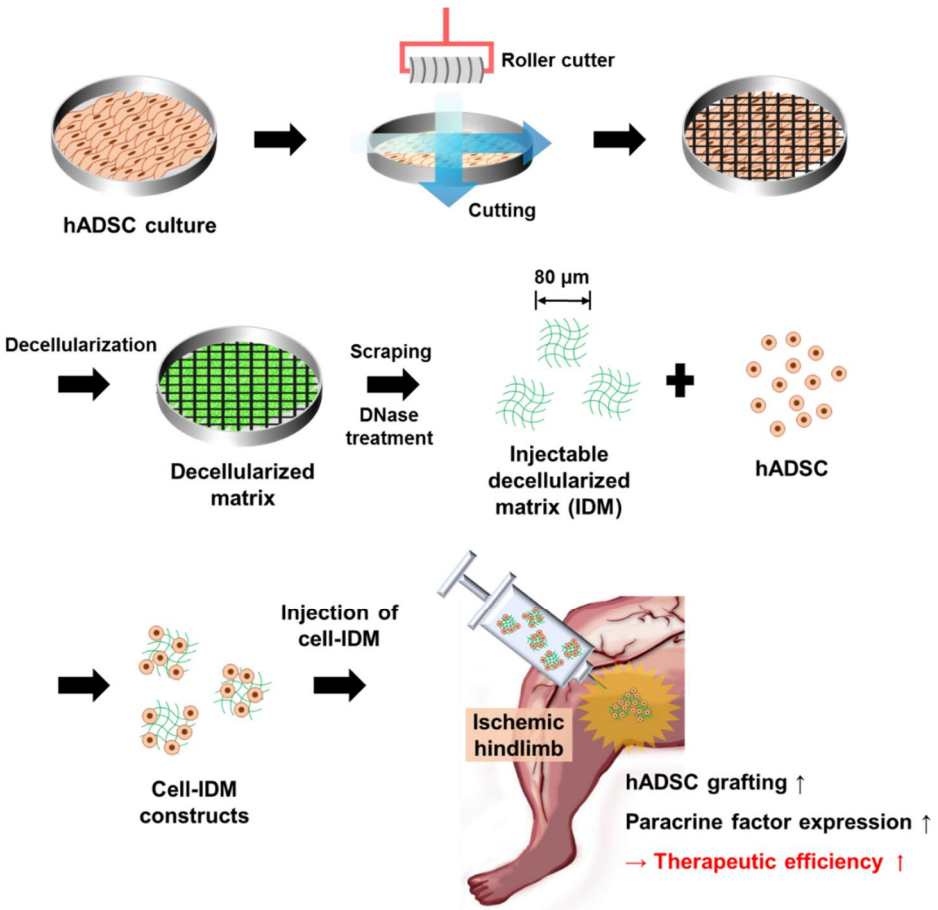


**Figure 4.1.** Schematic diagram of the injectable decellularized matrix (IDM) preparation and the *in vivo* experiment. Layers of confluently cultured cells were cut using a roller cutter, followed by decellularization and DNase treatment. Prior to cell injection, Cell-IDM constructs were formed by mixing IDMs and hADSCs. Injection of the Cell-IDM constructs would enhance therapeutic efficacy of hADSCs in mouse hindlimb ischemia model via improving the hADSC grafting and paracrine factor secretion of hADSCs, as compared to injection of hADSCs only.

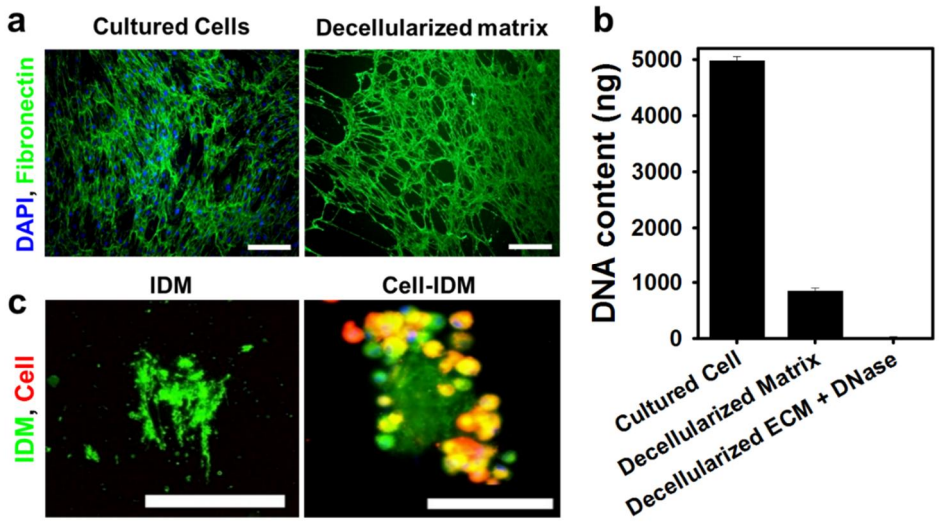


**Figure 4.2.** IDM characterization and Cell-IDM construct formation. (a) Before and after decellularization of cultured hADSC layer. ECM proteins were stained with anti-fibronectin antibody (green). Cell nuclei were stained with DAPI (blue). Scale bars = 100 μm. (b) DNA contents were determined before and after decellularization and DNase treatment of hADSC layer composed of $10^6$ cells and ECMs. (c) Before and after hADSC attachment to IDM. For cell attachment to IDM, a mixture of hADSCs and IDM was incubated for 30 min. IDM was stained with anti-fibronectin antibody (green). hADSCs were stained with PHK26 (red). Scale bars = 100 μm.

### 4.2.2. Optimization of incubation time for hADSC attachment to IDM

To optimize the incubation time for hADSC attachment to IDM, the percentage of cells attached to IDM was determined after incubation of a mixture of fluorescently labeled hADSCs and IDM in PBS for various time periods. The mixture ratio was $10^6$ cells to 4 mg IDM. The amount of IDM generated from $10^6$ hADSC culture was approximately 2mg. However, we used 4mg IDM per $10^6$ hADSCs, rather than 2mg IDM because the loss of ECM during the IDM fabrication process cannot provide sufficient amount of ECM for cell attachment. We used PBS to incubate the cell-IDM mixture because PBS is generally used to make cell suspension for cell implantation in clinics. The percentage of hADSCs attached to IDM was increased as the incubation time increased until 30 min (Figure 4.3a). The cell viability was maintained until 30 min and decreased at 60 min (Figure 4.3b). According to these results, we selected 30 min as the optimal incubation time of hADSC-IDM mixture and used for the following *in vitro* and *in vivo* experiments.

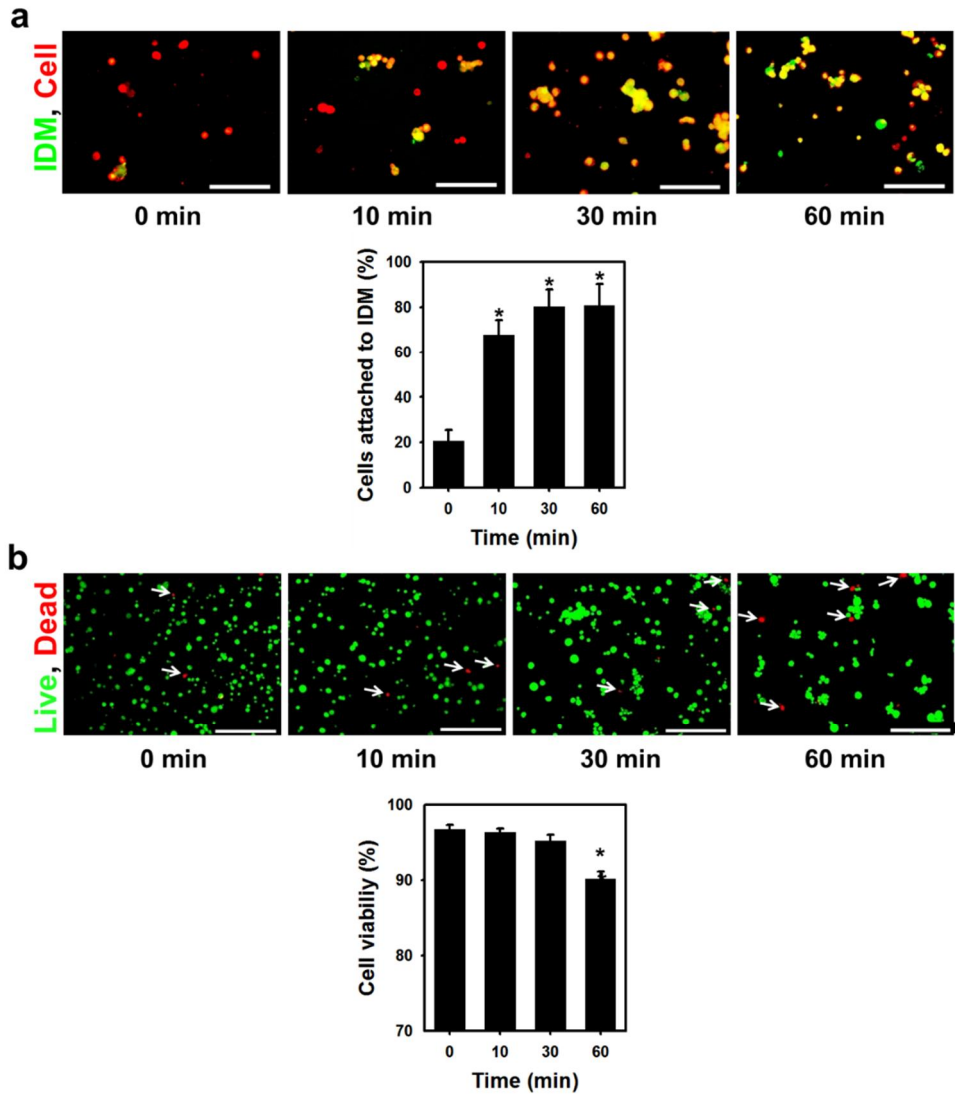


**Figure 4.3.** Optimization of incubation time of hADSCs/IDM mixture for hADSC adhesion to IDM. The mixture was composed of 4 mg IDM and $10^6$ hADSCs in PBS. (a) The percentage of cells attached to IDM was determined at various incubation time. IDM and cells were labeled with

coumarin (green) and PKH-26 (red), respectively. *$p < 0.05$ versus 0 min. n = 5 per group. (b) The viability of cells after incubation of hADSCs/IDM mixture for various time periods. Live and dead cells were labeled with FDA (green) and EB (red), respectively. *$p < 0.05$ versus 0 min. n = 5 per group.

### 4.2.3. *In vitro* prevention of hADSC anoikis by IDM

To determine whether hADSC attachment to IDM prevents anoikis of hADSCs under either cell-adhesion suppression condition or hypoxic condition, hADSCs were cultured on agarose-coated plates, which prevent cell adhesion to culture plates, under either normoxic (20% oxygen) or hypoxic condition (1% oxygen) that mimics the environment of ischemic tissue. Hypoxia in ischemic tissue promotes the reactive oxygen species production[108], which leads to prevention of implanted cell adhesion to ECM and subsequent anoikis of the implanted cells[109]. Thus, cell culture on agarose-coated plates under hypoxic condition can mimic the environment of ischemic tissue. The quantity of IDM mixed with hADSCs was 4 mg IDM per $10^6$ cells for the 1x IDM group and 10 mg IDM per $10^6$ cells for the 2.5x IDM group. Cell culture without IDM served as the control (the No IDM group). After 24 hr culture on agarose-coated plates under normoxic condition, the 1x IDM group and the 2.5x IDM group showed higher cell viability than the no IDM group (Figure 4.4a). There was no significant difference in the cell viability between the 1x IDM group and the 2.5x IDM group. This result indicates that hADSC

attachment to IDM can prevent anoikis of hADSCs under cell-adhesion suppression condition. Cell culture on agarose-coated plate under hypoxic condition for 24 hr also presented improved cell viability in the 1x IDM group and the 2.5x IDM group (Figure 4.4b). This result suggests that hADSC attachment to IDM may enhance hADSC viability following implantation into ischemic tissue. Since cell viability was not significantly different between the 1x IDM group and the 2.5x IDM group, 1x IDM was used in the following experiments. Next, qRT-PCR analysis was performed to examine whether hADSC-IDM constructs can prevent apoptosis of the hADSCs (Figure 4.5). hADSCs (the cell group) and hADSC-IDM constructs (the Cell-IDM group) were cultured on agarose-coated plates under hypoxic condition for 24 hr. Pro-apoptotic gene (BAX) expression was decreased and anti-apoptotic gene (Bcl-2) expression was increased in the Cell-IDM group as compared to the Cell group.

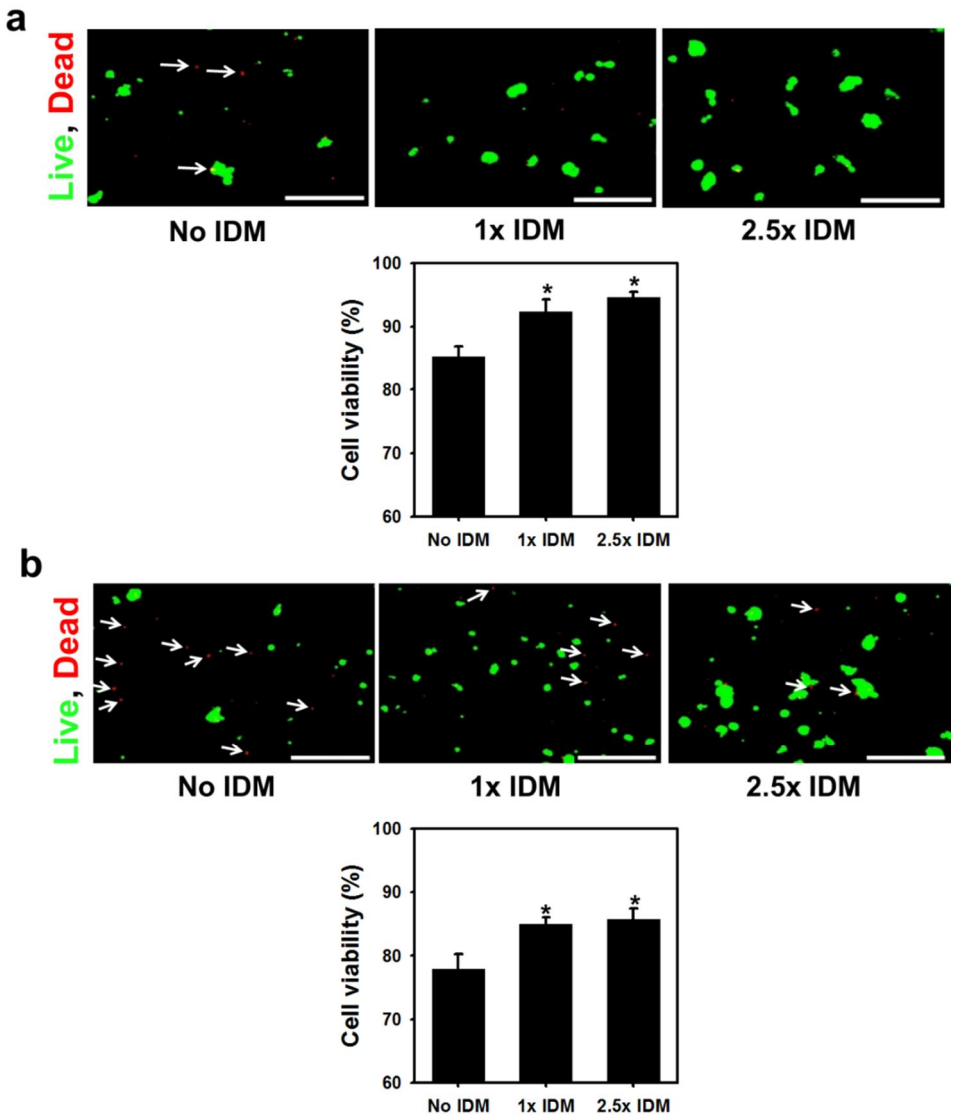


**Figure 4.4.** Reduced anoikis (i.e., cell death by loss of cell adhesion to ECMs) of hADSCs by Cell-IDM constructs. hADSCs were cultured in (a) normoxic (20% oxygen) or (b) hypoxic (1% oxygen) conditions for 24 hr on agarose-coated plates, which prevent cell adhesion to the dishes. The 1x

IDM group indicates constructs composed of 4 mg IDM and $10^6$ hADSCs. The 2.5x IDM group indicates constructs composed of 10 mg IDM and $10^6$ hADSCs. hADSCs without IDM served as the control. Live and dead cells were labeled with fluorescein diacetate (FDA, green) and ethidium bromide (EB, red), respectively. The cell viability was determined after 24 hr culture. *$p < 0.05$ versus the control group (No IDM). n = 5 per group.

### 4.2.4 *In vitro* upregulation of angiogenic factor expression

qRT-PCR analysis was performed to examine whether hADSC-IDM constructs can upregulate angiogenic paracrine of hADSCs (Figure 4.5). hADSCs (the Cell group) and hADSC-IDM constructs (the Cell-IDM group) were cultured on agarose-coated plates under hypoxic condition, which mimic the environment of ischemic tissue, for 24 hr. mRNA expression of angiogenic factors (VEGF and HGF) was upregulated in the Cell-IDM group as compared to the Cell group.

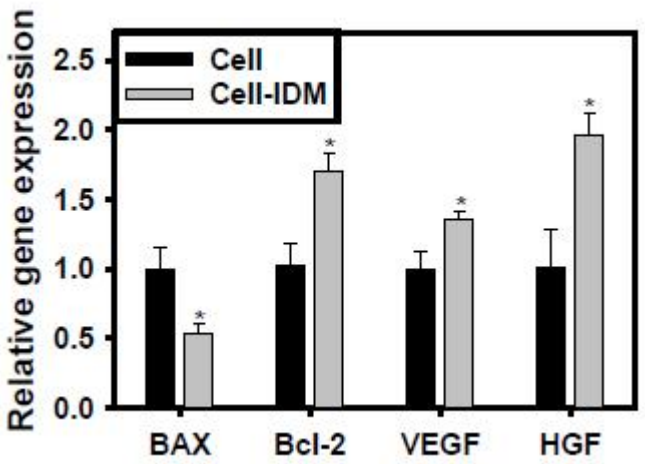


**Figure 4.5.** Reduced apoptotic signal expression and enhanced angiogenic paracrine factor expression in the Cell-IDM constructs 24 hr after culture in agarose-coated dishes under hypoxic (1% $O_2$) condition. Expressions of pro-apoptotic factor (BAX), anti-apoptotic factor (Bcl-2), and angiogenic factors (VEGF and HGF) were evaluated by real time-PCR analysis. *$p$ < 0.05 versus the Cell group. n = 4 per group.

### 4.2.5. *In vivo* engraftment of hADSCs implanted to ischemic tissue

Live imaging analysis was performed during 14 days after cell implantation to investigate *in vivo* engraftment of hADSCs injected to ischemic tissue. hADSCs were labeled with VivoTrack 680 prior to injection. The relative luminescence intensity of the Cell-IDM group was higher than that of the Cell group throughout the 14 day periods (Figure 4.6a). This result indicate that the engraftment of hADSCs implanted to ischemic tissue was enhanced by hADSC adhesion to IDM prior to injection. Immunohistochemistry was performed to examine apoptosis of the implanted hADSCs on day 7 (Figure 4.6b). Caspase-3 and HNA double stained cells indicate apoptotic hADSCs. The density of HNA-positive cells in the Cell-IDM group was higher than that of the Cell group, indicating that more hADSCs survived in the ischemic tissues by being implanted as hADSC-IDM constructs. Also, the density of Caspase-3 and HNA double stained cells was lower in the Cell-IDM group than in the Cell group, indicating that apoptosis of hADSCs implanted in the ischemic tissues decreased when cells were implanted as hADSC-IDM constructs.

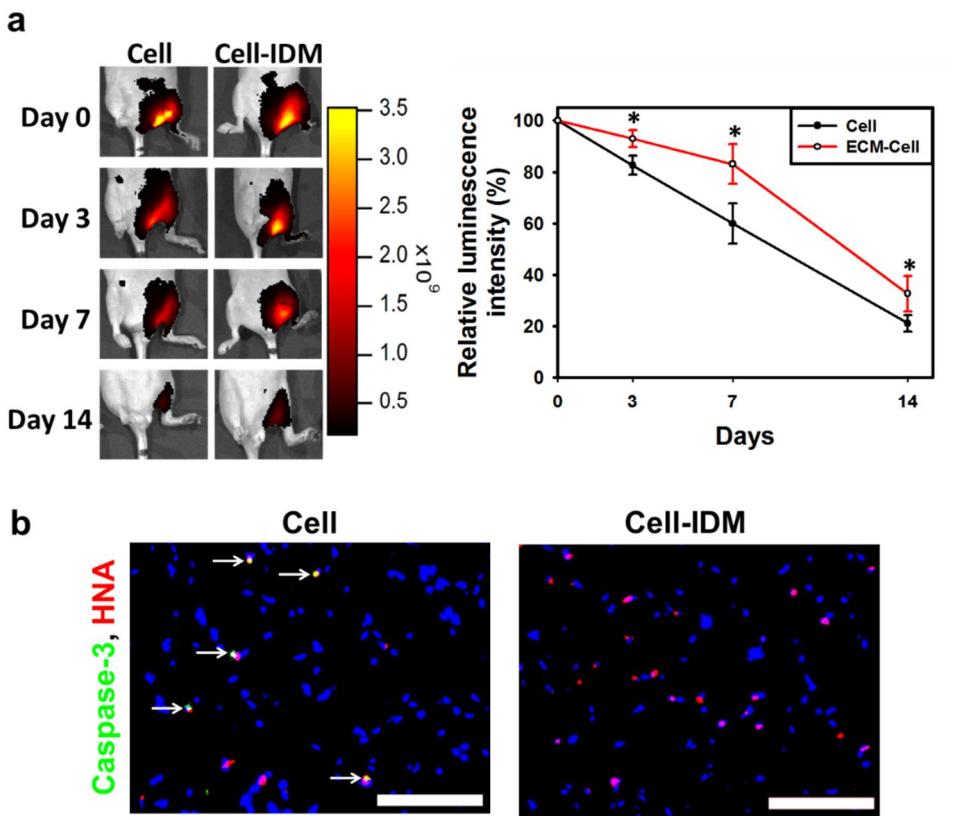


**Figure 4.6.** Enhanced hADSC grafting after injection of Cell-IDM constructs into hindlimb ischemic region in mice. (a) *In vivo* imaging of Vivo track 680-tagged hADSCs at day 0, 3, 7, and 14 days after implantation. The fluorescence intensity was quantified and normalized to that of each animal at day 0. * $p$ <0.05 versus the Cell group. n = 5 per group. (b) Immunohistochemistry staining for caspase-3 (green) and human nuclear antigen (HNA, red) at day 7. Cell nuclei were stained with DAPI (blue). Scale bars = 100 μm. White arrows indicate hADSCs

expressing caspase-3.

### 4.2.6. Angiogenic paracrine secretion in ischemic limbs

Western blot analysis for angiogenic protein expression was examined in the ischemic tissues of mouse hindlimb 7 days after hADSC implantation (Figure 4.7). VEGF, HGF, and SDF-1α expression was significantly increased in the Cell-IDM group as compared to the Cell group. Injection of IDM only was not used in the *in vivo* experiments because injection of ECM only did not show any therapeutic effects in a previous study.[110]

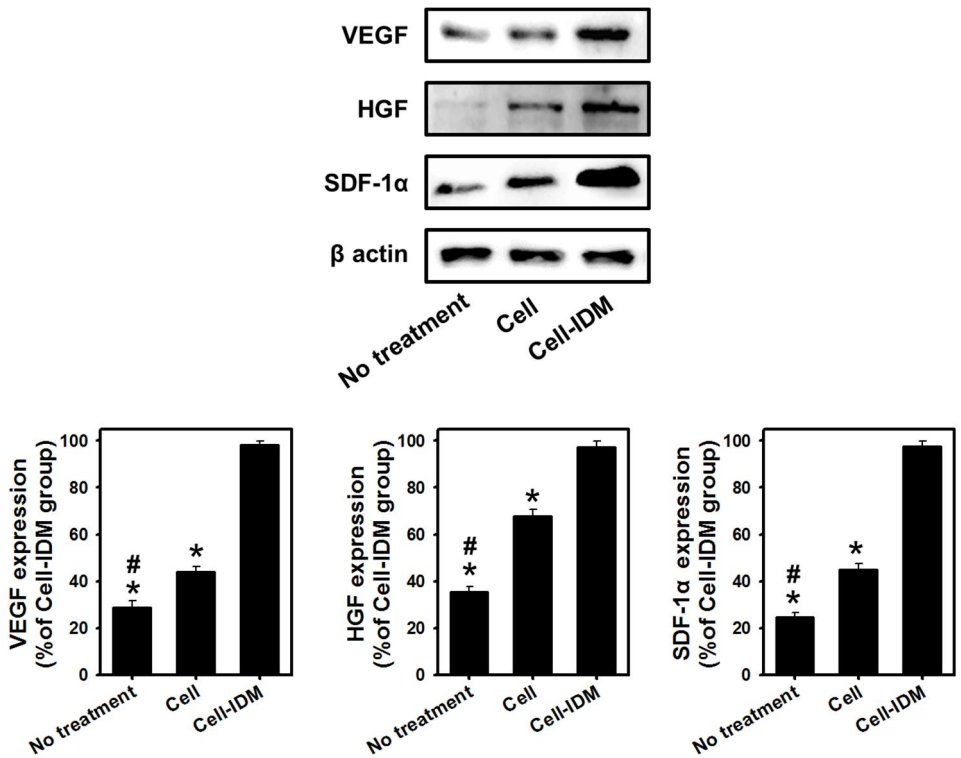


**Figure 4.7.** Enhanced expression of angiogenic factors (VEGF, HGF, and SDF-1α) in hindlimb ischemic regions in mice by injection of Cell-IDM constructs, as evaluated by western blot analysis of the ischemic tissues at day 7. *$p < 0.05$ versus the Cell-IDM group. #$p < 0.05$ versus the Cell group. n = 4 per group.

### 4.2.7. Microvessel density in ischemic limbs

Immunofluorescent staining using antibodies against CD31 and SM α-actin was performed to evaluate microvessel density in the ischemic hindlimbs 28 days after hADSC implantation (Figure 4.8a). SM α-actin- and CD31-positive microvessel density in the Cell-IDM was significantly higher than those of the other groups. Western blotting analysis of the ischemic tissues also showed that CD31 and SM α-actin expression was significantly increased in the Cell-IDM group (Figure 4.8b).

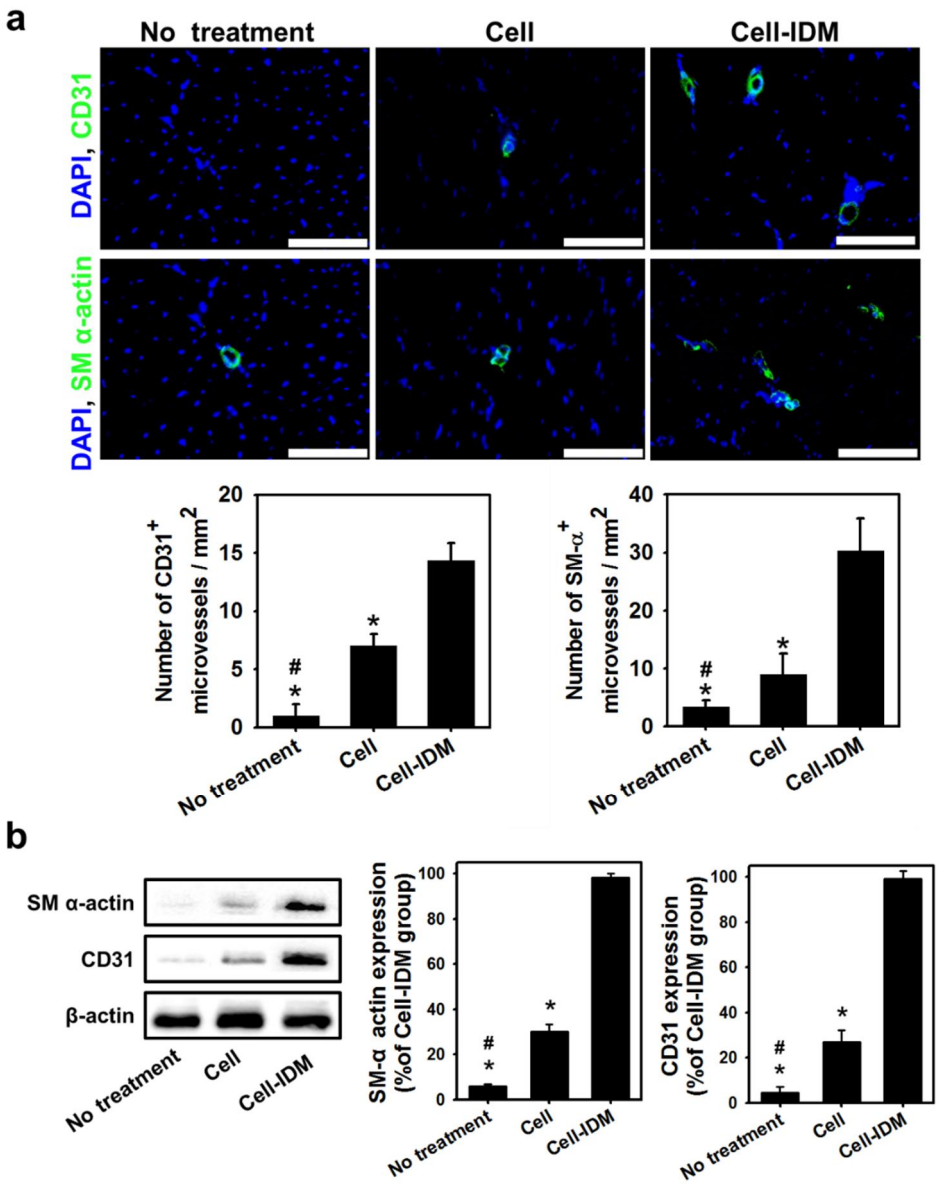


**Figure 4.8.** Enhanced microvessel formation in hindlimb ischemic regions in mice by injection of Cell-IDM constructs. (a) Immunohistochemistry for SM α-actin-positive microvessels (green) and CD31-positive microvessels

(green) in the ischemic region at 28 days after treatment. Scale bars = 100 μm. Blue indicates nuclei stained with DAPI. *$p < 0.05$ versus the Cell-IDM group. #$p < 0.05$ versus the Cell group. n = 10 per group. (b) Western blot analysis for SM α-actin and CD31 expression in the ischemic regions of mouse hindlimbs. *$p < 0.05$ versus the Cell-IDM group. #$p < 0.05$ versus the Cell group. n = 4 per group.

### 4.2.8. Blood perfusion in the ischemic limb

Every 7 days after the hindlimb ischemia treatments, blood perfusion rate of the ischemic limbs was monitored. In the Cell-IDM group, the blood perfusion rate was significantly higher than that of the other groups on day 21 and 28 (Figure 4.9 a and b). H&E and Masson's trichrome staining showed less tissue necrosis and fibrosis in the Cell-IDM group than that of the other groups (Figure 4.9c).

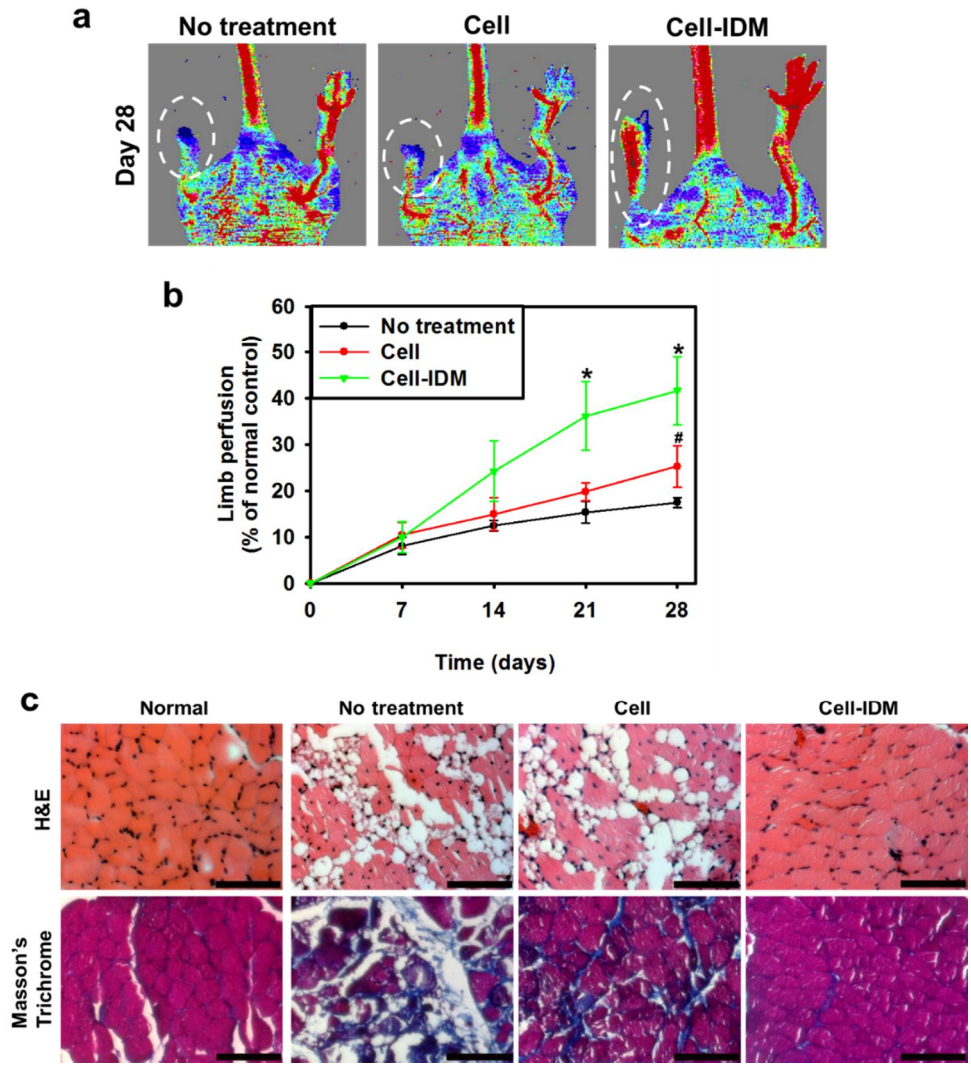


**Figure 4.9.** Improved blood perfusion and decreased fibrosis in the ischemic region of mouse hindlimbs by Cell-IDM implantation. (a) Representative images of ischemic limbs 28 days after treatment. The dotted areas indicate ischemic limbs. (b) Blood perfusion of the ischemic limbs was monitored for 28 days (n = 12 per group). *$p < 0.05$ versus both

the cell group and the no treatment group, #$p < 0.05$ versus the no treatment group. (c) Histological evaluation of the ischemic region. Tissues in the ischemic regions were stained with H&E (upper panel) and Masson's trichrome (lower panel) at 28 days after treatment. Scale bars = 100 μm.

## 4.3. Discussions

ECM can regulate stem cell behaviors including survival and differentiation.[111-113] Anoikis is initiated when interactions between stem cells and ECM are cut off.[114] For both animal studies and clinical applications, stem cells are commonly harvested from culture plates for implantation through proteolytic enzyme treatment. Following the treatment, interactions between cells and ECM are lost and adhesion-related survival signals are downregulated, which causes cell anoikis.[115] In addition, harsh microenvironments in the ischemic tissue causes massive apoptosis of stem cells implanted to the ischemic tissue.[109, 116] The poor engraftment of implanted cells deteriorates the therapeutic efficacy of the stem cells, which is a critical limitation of current stem cell therapies for ischemia disease.[5]

This study shows that engraftment of hADSCs implanted to ischemic tissue can be improved by hADSC adhesion to IDM prior to implantation. It has previously been shown that survival of stem cells implanted to ischemic tissue is determined by the extent of ischemia in the region of initial cell adhesion of implanted stem cells.[117] In agreement with the

previous study, our *in vitro* data showed that the viability of cultured hADSCs decreased when hypoxia was induced (Figure 4 a and b, the no IDM group). hADSC attachment to IDM significantly improved the viability in culture under either cell-adhesion suppression condition of hypoxic condition (Figure 4.4). This suggests that hADSCs implanted to ischemic tissue, which has microenvironments of cell-adhesion suppression condition by reactive oxygen species[118] and low oxygen concentration, would exhibit improved cell survival by implantation in the form of hADSC-IDM constructs. Indeed, our *in vivo* data showed that engraftment of hADSCs in ischemic tissue was enhanced by implantation of hADSC-IDM constructs (Figure 4.6). The fabricated IDM was approximately 80 μm (figure 4.2), which enabled implantation of hADSC-IDM constructs through injection.

The percentage of hADSCs adherent to IDM immediately after mixing hADSCs and IDM was not 0% but 20% (Figure 4.3a). This was probably because the hADSC density in the mixture was very high ($10^7$ cells/ml, $10^6$ cells per 100 μl PBS) and instant cell attachment to fibronectin of IDM occurred.[40] In the *in vitro* experiment for optimization of incubation time for hADSC attachment to IDM, the cell viability was maintained until 30 min in the cell-IDM group, but decreased at 60 min, a short time period

(Figure 3b). This was probably because cells were suspended in nutrient-depleted PBS and apoptosis may have occurred by nutrient depletion.[119-120]

This study also shows that therapeutic efficacy of hADSCs can be improved by implantation of hADSC-IDM constructs. The improved therapeutic efficacy may be attributed to improved hADSC engraftment by implantation in the form of hADSC-IDM constructs. The main therapeutic mechanism of MSC therapy for ischemic diseases is paracrine action of angiogenic factors secreted from the implanted MSCs.[121] If more MSCs are engrafted following MSC implantation, more soluble factors would be produced from the implanted MSCs. Indeed, our *in vivo* data showed that injection of hADSC-IDM resulted in higher engraftment of hADSCs (Figure 4.6) and greater secretion of angiogenic factors (Figure 4.7).

# Chapter 5.

# Conclusions

The present study is the report on the enhancing therapeutic angiogenesis in mouse hindlimb ischemia model by usage of electrical stimulation derived from solar cell and injectable decellularixed extracellular matrix (IDM) for stem cell transplantation.

In chapter 3, the solar-cell-based device was designed to control cell behavior and stimulate therapeutic angiogenesis in a mouse ischemic hindlimb. The device successfully converted light energy into electrical energy and generated ES. ES induced cell migration and promoted the secretion of angiogenic paracrine factors. Furthermore, use of the solar cell device led to significant increase in the number of capillaries and arterioles at the ischemic region, and prevented muscle necrosis and loss of the ischemic limb.

In the chapter 4, injectable decellularized matrix (IDM) was investigated and examined whether the IDM can enhance transplanted cell grafting and therapeutic efficacy. In an *in vitro* experiment, IDM and ADSC complex (Cell-IDM) enhanced cell viability and upregulation of angiogenic paracrine factors. To evaluate the therapeutic efficacy *in vivo*, Cell-IDM was implanted into the ischemic region of a mouse hindlimb. Transplantation of Cell-IDM induced significant increase in the number of capillaries and arterioles at the ischemic region, and prevented muscle

necrosis.

The result of this study may be applicable for the enhancing and optimizing therapeutic angiogenesis in both cell transplantation model and *in vivo* implantable device model. Moreover, this study provided a disposable and easily usable and implantable ES-generating solar cell device and easily applicable developed stem cell transplantation method to treat angiogenic disease.

# References


1. Folkman, J., Angiogenesis-retrospect and outlook. *Exs* **1992,** *61*, 4-13.

2. Papetti, M.; Herman, I. M., Mechanisms of normal and tumor-derived angiogenesis. *American Journal of Physiology-Cell Physiology* **2002,** *282* (5), C947-C970.

3. Presta, M.; Dell'Era, P.; Mitola, S.; Moroni, E.; Ronca, R.; Rusnati, M., Fibroblast growth factor/fibroblast growth factor receptor system in angiogenesis. *Cytokine & growth factor reviews* **2005,** *16* (2), 159-178.

4. Otrock, Z. K.; Mahfouz, R. A.; Makarem, J. A.; Shamseddine, A. I., Understanding the biology of angiogenesis: review of the most important molecular mechanisms. *Blood Cells, Molecules, and Diseases* **2007,** *39* (2), 212-220.

5. Mamidi, M. K.; Pal, R.; Dey, S.; Abdullah, B. J. J. B.; Zakaria, Z.; Rao, M. S.; Das, A. K., Cell therapy in critical limb ischemia: current developments and future progress. *Cytotherapy* **2012,** *14* (8), 902-916.

6. Gupta, R.; Losordo, D. W., Cell therapy for critical limb ischemia. Am Heart Assoc: 2011.

7. Lawall, H.; Bramlage, P.; Amann, B., Stem cell and progenitor cell therapy in peripheral artery disease. *Thromb Haemost* **2010,** *103* (4), 696-709.

8. Burns, T. C.; Verfaillie, C. M.; Low, W. C., Stem cells for ischemic brain injury: a critical review. *Journal of Comparative Neurology* **2009,** *515* (1), 125-144.

9. Teraa, M.; Sprengers, R. W.; van der Graaf, Y.; Peters, C. E.; Moll, F. L.; Verhaar, M. C., Autologous Bone Marrow–Derived Cell Therapy in Patients With Critical Limb Ischemia: A Meta-Analysis of Randomized Controlled Clinical Trials. *Annals of surgery* **2013,** *258* (6), 922-929.

10. Lindvall, O.; Kokaia, Z., Stem cells for the treatment of neurological disorders. *Nature* **2006,** *441* (7097), 1094-1096.

11. Burchfield, J. S.; Dimmeler, S., Role of paracrine factors in stem and progenitor cell mediated cardiac repair and tissue fibrosis. *Fibrogenesis & tissue repair* **2008,** *1* (1), 4.

12. Hill, E.; Boontheekul, T.; Mooney, D. J., Regulating activation of transplanted cells controls tissue regeneration. *Proceedings of the National Academy of Sciences of the United States of America* **2006,** *103* (8), 2494-2499.

13. Robey, T. E.; Saiget, M. K.; Reinecke, H.; Murry, C. E., Systems approaches to preventing transplanted cell death in cardiac repair. *Journal of molecular and cellular cardiology* **2008,** *45* (4), 567-581.

14. Zhang, M.; Methot, D.; Poppa, V.; Fujio, Y.; Walsh, K.; Murry, C. E., Cardiomyocyte grafting for cardiac repair: graft cell death and anti-death strategies. *Journal of molecular and cellular cardiology* **2001,** *33* (5), 907-921.

15. Robinson, K. R., The responses of cells to electrical fields: a review. *J Cell Biol* **1985,** *101* (6), 2023-2027.

16. Hang, J.; Kong, L.; Gu, J.; Adair, T., VEGF gene expression is upregulated in electrically stimulated rat skeletal muscle. *American Journal of Physiology: Heart and Circulatory Physiology* **1995,** *269* (5), 1827-1831.

17. Tandon, N.; Cannizzaro, C.; Chao, P.-H. G.; Maidhof, R.; Marsano, A.; Au, H. T. H.; Radisic, M.; Vunjak-Novakovic, G., Electrical stimulation systems for cardiac tissue engineering. *Nature protocols* **2009,** *4* (2), 155-173.

18. Balint, R.; Cassidy, N. J.; Cartmell, S. H., Electrical stimulation: a novel tool for tissue engineering. *Tissue Eng., Part B* **2012,** *19* (1), 48-57.

19. McCaig, C. D.; Zhao, M., Physiological electrical fields modify cell behaviour. *Bioessays* **1997,** *19* (9), 819-826.

20. Zhao, M.; Bai, H.; Wang, E.; Forrester, J. V.; McCaig, C. D., Electrical stimulation directly induces pre-angiogenic responses in vascular endothelial cells by signaling through VEGF receptors. *Journal of cell science* **2004,** *117* (3), 397-

405.

21. Song, B.; Zhao, M.; Forrester, J. V.; McCaig, C. D., Electrical cues regulate the orientation and frequency of cell division and the rate of wound healing in vivo. *Proceedings of the National Academy of Sciences of the United States of America* **2002,** *99* (21), 13577-13582.

22. Nuccitelli, R., Endogenous ionic currents and DC electric fields in multicellular animal tissues. *Bioelectromagnetics* **1992,** *13* (S1), 147-157.

23. Bhang, S. H.; Jang, W. S.; Han, J.; Yoon, J. K.; La, W. G.; Lee, E.; Kim, Y. S.; Shin, J. Y.; Lee, T. J.; Baik, H. K., Zinc Oxide Nanorod-Based Piezoelectric Dermal Patch for Wound Healing. *Adv. Funct. Mater.* **2017,** *27* (1), 1603491.

24. Hynes, R. O., Integrins: bidirectional, allosteric signaling machines. *Cell* **2002,** *110* (6), 673-687.

25. Berrier, A. L.; Yamada, K. M., Cell–matrix adhesion. *Journal of cellular physiology* **2007,** *213* (3), 565-573.

26. Legate, K. R.; Wickström, S. A.; Fässler, R., Genetic and cell biological analysis of integrin outside-in signaling. *Genes & development* **2009,** *23* (4), 397-418.

27. Discher, D. E.; Mooney, D. J.; Zandstra, P. W., Growth factors, matrices, and forces combine and control stem cells. *Science* **2009,** *324* (5935), 1673-1677.

28. Geiger, B.; Spatz, J. P.; Bershadsky, A. D., Environmental sensing through focal adhesions. *Nature reviews Molecular cell biology* **2009,** *10* (1), 21-33.

29. Shafiq, M.; Jung, Y.; Kim, S. H., Insight on stem cell preconditioning and instructive biomaterials to enhance cell adhesion, retention, and engraftment for tissue repair. *Biomaterials* **2016,** *90*, 85-115.

30. Bhang, S. H.; Lee, T.-J.; La, W.-G.; Kim, D.-I.; Kim, B.-S., Delivery of fibroblast growth factor 2 enhances the viability of cord blood-derived mesenchymal stem cells transplanted to ischemic limbs. *J. Biosci. Bioeng.* **2011,** *111* (5), 584-589.

31. Deuse, T.; Peter, C.; Fedak, P. W.; Doyle, T.; Reichenspurner, H.; Zimmermann, W. H.; Eschenhagen, T.; Stein, W.; Wu, J. C.; Robbins, R. C., Hepatocyte growth factor or vascular endothelial growth factor gene transfer maximizes mesenchymal stem cell–based myocardial salvage after acute myocardial infarction. *Circulation* **2009,** *120* (11 suppl 1), S247-S254.

32. Madonna, R.; Taylor, D. A.; Geng, Y.-J.; De Caterina, R.; Shelat, H.; Perin, E. C.; Willerson, J. T., Transplantation of mesenchymal cells rejuvenated by the overexpression of telomerase and myocardin promotes revascularization and tissue repair in a murine model of hindlimb ischemia. *Circulation research* **2013**, CIRCRESAHA. 113.301690.

33. Jay, S. M.; Shepherd, B. R.; Bertram, J. P.; Pober, J. S.; Saltzman, W. M., Engineering of multifunctional gels integrating highly efficient growth factor delivery with endothelial cell transplantation. *The FASEB Journal* **2008,** *22* (8), 2949-2956.

34. Fitzpatrick, J. R.; Frederick, J. R.; McCormick, R. C.; Harris, D. A.; Kim, A.-Y.; Muenzer, J. R.; Gambogi, A. J.; Liu, J. P.; Paulson, E. C.; Woo, Y. J., Tissue-engineered pro-angiogenic fibroblast scaffold improves myocardial perfusion and function and limits ventricular remodeling after infarction. *The Journal of thoracic and cardiovascular surgery* **2010,** *140* (3), 667-676.

35. Baek, K.; Tu, C.; Zoldan, J.; Suggs, L. J., Gene transfection for stem cell therapy. *Current Stem Cell Reports* **2016,** *2* (1), 52-61.

36. Nowakowski, A.; Andrzejewska, A.; Janowski, M.; Walczak, P.; Lukomska, B., Genetic engineering of stem cells for enhanced therapy. *Acta Neurobiol Exp (Wars)* **2013,** *73* (1), 1-18.

37. Bhang, S. H.; Lim, J. S.; Choi, C. Y.; Kwon, Y. K.; Kim, B.-S., The behavior of neural stem cells on biodegradable synthetic polymers. *Journal of Biomaterials Science, Polymer Edition* **2007,** *18* (2), 223-239.

38. Lutolf, M.; Hubbell, J., Synthetic biomaterials as instructive extracellular microenvironments for morphogenesis in tissue engineering. *Nat. Biotechnol.*

**2005,** *23* (1), 47-55.

39. Mooney, D. J.; Vandenburgh, H., Cell delivery mechanisms for tissue repair. *Cell stem cell* **2008,** *2* (3), 205-213.

40. Seif-Naraghi, S. B.; Singelyn, J. M.; Salvatore, M. A.; Osborn, K. G.; Wang, J. J.; Sampat, U.; Kwan, O. L.; Strachan, G. M.; Wong, J.; Schup-Magoffin, P. J., Safety and efficacy of an injectable extracellular matrix hydrogel for treating myocardial infarction. *Science translational medicine* **2013,** *5* (173), 173ra25-173ra25.

41. DeQuach, J. A.; Lin, J. E.; Cam, C.; Hu, D.; Salvatore, M. A.; Sheikh, F.; Christman, K. L., Injectable skeletal muscle matrix hydrogel promotes neovascularization and muscle cell infiltration in a hindlimb ischemia model. *European cells & materials* **2012,** *23*, 400.

42. Mebarki, M.; Coquelin, L.; Layrolle, P.; Battaglia, S.; Tossou, M.; Hernigou, P.; Rouard, H.; Chevallier, N., Enhanced human bone marrow mesenchymal stromal cell adhesion on scaffolds promotes cell survival and bone formation. *Acta Biomaterialia* **2017,** *59*, 94-107.

43. He, F.; Liu, X.; Xiong, K.; Chen, S.; Zhou, L.; Cui, W.; Pan, G.; Luo, Z.-P.; Pei, M.; Gong, Y., Extracellular matrix modulates the biological effects of melatonin in mesenchymal stem cells. *Journal of Endocrinology* **2014,** *223* (2), 167-180.

44. Yamamoto, N.; Akamatsu, H.; Hasegawa, S.; Yamada, T.; Nakata, S.; Ohkuma, M.; Miyachi, E.-I.; Marunouchi, T.; Matsunaga, K., Isolation of multipotent stem cells from mouse adipose tissue. *J. Dermatol. Sci.* **2007,** *48* (1), 43-52.

45. Hedayatpour, A.; Ragerdi, I.; Pasbakhsh, P.; Kafami, L.; Atlasi, N.; Mahabadi, V. P.; Ghasemi, S.; Reza, M., Promotion of remyelination by adipose mesenchymal stem cell transplantation in a cuprizone model of multiple sclerosis. *Cell J.* **2013,** *15* (2), 142.

46. Yin, L.; Zhu, Y.; Yang, J.; Ni, Y.; Zhou, Z.; Chen, Y.; Wen, L., Adipose

tissue-derived mesenchymal stem cells differentiated into hepatocyte-like cells in vivo and in vitro. *Mol. Med. Rep.* **2015,** *11* (3), 1722-1732.

47. Seemann, I.; te Poele, J. A.; Hoving, S.; Stewart, F. A., Mouse bone marrow-derived endothelial progenitor cells do not restore radiation-induced microvascular damage. *ISRN Cardiol.* **2014,** *2014*.

48. Sangidorj, O.; Yang, S. H.; Jang, H. R.; Lee, J. P.; Cha, R.-h.; Kim, S. M.; Lim, C. S.; Kim, Y. S., Bone marrow-derived endothelial progenitor cells confer renal protection in a murine chronic renal failure model. *Am. J. Physiol.: Renal, Fluid Electrolyte Physiol.* **2010,** *299* (2), F325-F335.

49. Blanco-Bose, W. E.; Yao, C.-C.; Kramer, R. H.; Blau, H. M., Purification of mouse primary myoblasts based on α7 integrin expression. *Exp. Cell Res.* **2001,** *265* (2), 212-220.

50. Bhang, S. H.; Lee, S.; Shin, J.-Y.; Lee, T.-J.; Jang, H.-K.; Kim, B.-S., Efficacious and clinically relevant conditioned medium of human adipose-derived stem cells for therapeutic angiogenesis. *Molecular Therapy* **2014,** *22* (4), 862-872.

51. Cho, S.-W.; Moon, S.-H.; Lee, S.-H.; Kang, S.-W.; Kim, J.; Lim, J. M.; Kim, H.-S.; Kim, B.-S.; Chung, H.-M., Improvement of postnatal neovascularization by human embryonic stem cell–derived endothelial-like cell transplantation in a mouse model of hindlimb ischemia. *Circulation* **2007,** *116* (21), 2409-2419.

52. Gil, C.-H.; Ki, B.-S.; Seo, J.; Choi, J.-J.; Kim, H.; Kim, I.-G.; Jung, A.-R.; Lee, W.-Y.; Choi, Y.; Park, K., Directing human embryonic stem cells towards functional endothelial cells easily and without purification. *Tissue Eng. Regener. Med.* **2016,** *13* (3), 274-283.

53. Jang, H. K.; Kim, B. S.; Han, J.; Yoon, J. K.; Lee, J. R.; Jeong, G. J.; Shin, J. Y., Therapeutic angiogenesis using tumor cell-conditioned medium. *Biotechnology progress* **2016,** *32* (2), 456-464.

54. Shin, J.-Y.; Yoon, J.-K.; Noh, M. K.; Bhang, S. H.; Kim, B.-S., Enhancing Therapeutic Efficacy and Reducing Cell Dosage in Stem Cell

Transplantation Therapy for Ischemic Limb Diseases by Modifying the Cell Injection Site. *Tissue Eng., Part A* **2016,** *22* (3-4), 349-362.

55. Tateishi-Yuyama, E.; Matsubara, H.; Murohara, T.; Ikeda, U.; Shintani, S.; Masaki, H.; Amano, K.; Kishimoto, Y.; Yoshimoto, K.; Akashi, H., Therapeutic angiogenesis for patients with limb ischaemia by autologous transplantation of bone-marrow cells: a pilot study and a randomised controlled trial. *The Lancet* **2002,** *360* (9331), 427-435.

56. Huikuri, H. V.; Kervinen, K.; Niemelä, M.; Ylitalo, K.; Säily, M.; Koistinen, P.; Savolainen, E.-R.; Ukkonen, H.; Pietilä, M.; Airaksinen, J. K., Effects of intracoronary injection of mononuclear bone marrow cells on left ventricular function, arrhythmia risk profile, and restenosis after thrombolytic therapy of acute myocardial infarction. *European heart journal* **2008,** *29* (22), 2723-2732.

57. Meyer, G. P.; Wollert, K. C.; Lotz, J.; Pirr, J.; Rager, U.; Lippolt, P.; Hahn, A.; Fichtner, S.; Schaefer, A.; Arseniev, L., Intracoronary bone marrow cell transfer after myocardial infarction: 5-year follow-up from the randomized-controlled BOOST trial. *European heart journal* **2009,** *30* (24), 2978-2984.

58. Assmus, B.; Rolf, A.; Erbs, S.; Elsässer, A.; Haberbosch, W.; Hambrecht, R.; Tillmanns, H.; Yu, J.; Corti, R.; Mathey, D. G., Clinical outcome 2 years after intracoronary administration of bone marrow-derived progenitor cells in acute myocardial infarction. *Circulation: Heart Failure* **2010,** *3*, 89-96.

59. Assmus, B.; Schächinger, V.; Teupe, C.; Britten, M.; Lehmann, R.; Döbert, N.; Grünwald, F.; Aicher, A.; Urbich, C.; Martin, H., Transplantation of progenitor cells and regeneration enhancement in acute myocardial infarction (TOPCARE-AMI). *Circulation* **2002,** *106* (24), 3009-3017.

60. Han, J.; Kim, B.; Shin, J.-Y.; Ryu, S.; Noh, M.; Woo, J.; Park, J.-S.; Lee, Y.; Lee, N.; Hyeon, T., Iron oxide nanoparticle-mediated development of cellular gap junction crosstalk to improve mesenchymal stem cells' therapeutic efficacy for myocardial infarction. *ACS nano* **2015,** *9* (3), 2805-2819.

61. Hodgson, D. M.; Behfar, A.; Zingman, L. V.; Kane, G. C.; Perez-Terzic, C.; Alekseev, A. E.; Pucéat, M.; Terzic, A., Stable benefit of embryonic stem cell therapy in myocardial infarction. *American Journal of Physiology: Heart and Circulatory Physiology* **2004,** *287* (2), 471-479.

62. Min, J.-Y.; Yang, Y.; Converso, K. L.; Liu, L.; Huang, Q.; Morgan, J. P.; Xiao, Y.-F., Transplantation of embryonic stem cells improves cardiac function in postinfarcted rats. *Journal of Applied Physiology* **2002,** *92* (1), 288-296.

63. Xie, C.-Q.; Zhang, J.; Xiao, Y.; Zhang, L.; Mou, Y.; Liu, X.; Akinbami, M.; Cui, T.; Chen, Y. E., Transplantation of human undifferentiated embryonic stem cells into a myocardial infarction rat model. *Stem Cells Dev.* **2007,** *16* (1), 25-30.

64. Ye, L.; Chang, Y.-H.; Xiong, Q.; Zhang, P.; Zhang, L.; Somasundaram, P.; Lepley, M.; Swingen, C.; Su, L.; Wendel, J. S., Cardiac repair in a porcine model of acute myocardial infarction with human induced pluripotent stem cell-derived cardiovascular cells. *Cell stem cell* **2014,** *15* (6), 750-761.

65. Templin, C.; Zweigerdt, R.; Schwanke, K.; Olmer, R.; Ghadri, J.-R.; Emmert, M. Y.; Müller, E.; Küest, S. M.; Cohrs, S.; Schibli, R., Transplantation and tracking of human induced pluripotent stem cells in a pig model of myocardial infarction: assessment of cell survival, engraftment and distribution by hybrid SPECT-CT imaging of sodium iodide symporter trangene expression. *Circulation* **2012,** *126*, 430-439.

66. Xiong, Q.; Ye, L.; Zhang, P.; Lepley, M.; Tian, J.; Li, J.; Zhang, L.; Swingen, C.; Vaughan, J. T.; Kaufman, D. S., Functional consequences of human induced pluripotent stem cells therapy: myocardial ATP turnover rate in the in vivo swine hearts with post-infarction remodeling. *Circulation* **2013,** *127*, 997-1008.

67. He, N.; Xu, Y.; Du, W.; Qi, X.; Liang, L.; Wang, Y.; Feng, G.; Fan, Y.; Han, Z.; Kong, D., Extracellular matrix can recover the downregulation of adhesion molecules after cell detachment and enhance endothelial cell

engraftment. *Scientific reports* **2015,** *5*.

68. Zeng, L.; Hu, Q.; Wang, X.; Mansoor, A.; Lee, J.; Feygin, J.; Zhang, G.; Suntharalingam, P.; Boozer, S.; Mhashilkar, A., Bioenergetic and functional consequences of bone marrow–derived multipotent progenitor cell transplantation in hearts with postinfarction left ventricular remodeling. *Circulation* **2007,** *115* (14), 1866-1875.

69. Ranganath, S. H.; Levy, O.; Inamdar, M. S.; Karp, J. M., Harnessing the mesenchymal stem cell secretome for the treatment of cardiovascular disease. *Cell stem cell* **2012,** *10* (3), 244-258.

70. Menasché, P., Stem cells for clinical use in cardiovascular medicine. *Thromb. Haemostasis* **2005,** *94*, 697-701.

71. Bigland-Ritchie, B.; Jones, D.; Woods, J., Excitation frequency and muscle fatigue: electrical responses during human voluntary and stimulated contractions. *Exp. Neurol.* **1979,** *64* (2), 414-427.

72. Sidney, L. E.; Branch, M. J.; Dunphy, S. E.; Dua, H. S.; Hopkinson, A., Concise review: evidence for CD34 as a common marker for diverse progenitors. *Stem cells* **2014,** *32* (6), 1380-1389.

73. Ragnarsson, K., Functional electrical stimulation after spinal cord injury: current use, therapeutic effects and future directions. *Spinal cord* **2008,** *46* (4), 255-274.

74. Zhang, P.; Liu, Z.-T.; He, G.-X.; Liu, J.-P.; Feng, J., Low-voltage direct-current stimulation is safe and promotes angiogenesis in rabbits with myocardial infarction. *Cell biochemistry and biophysics* **2011,** *59* (1), 19-27.

75. Ud-Din, S.; Sebastian, A.; Giddings, P.; Colthurst, J.; Whiteside, S.; Morris, J.; Nuccitelli, R.; Pullar, C.; Baguneid, M.; Bayat, A., Angiogenesis is induced and wound size is reduced by electrical stimulation in an acute wound healing model in human skin. *PLoS one* **2015,** *10* (4), e0124502.

76. Kloth, L. C., Electrical stimulation for wound healing: a review of evidence from in vitro studies, animal experiments, and clinical trials. *Int. J.*

*Lower Extremity Wounds* **2005,** *4* (1), 23-44.

77. Patterson, C.; Runge, M. S., Therapeutic angiogenesis. Am Heart Assoc: 1999; Vol. 99, pp 2614-2616.

78. Zhao, Z.; Qin, L.; Reid, B.; Pu, J.; Hara, T.; Zhao, M., Directing migration of endothelial progenitor cells with applied DC electric fields. *Stem cell research* **2012,** *8* (1), 38-48.

79. Mycielska, M. E.; Djamgoz, M. B., Cellular mechanisms of direct-current electric field effects: galvanotaxis and metastatic disease. *Journal of cell science* **2004,** *117* (9), 1631-1639.

80. Bai, H.; Forrester, J. V.; Zhao, M., DC electric stimulation upregulates angiogenic factors in endothelial cells through activation of VEGF receptors. *Cytokine* **2011,** *55* (1), 110-115.

81. Liu, Q.; Song, B., Electric field regulated signaling pathways. *Int. J. Biochem. Cell Biol.* **2014,** *55*, 264-268.

82. Serena, E.; Figallo, E.; Tandon, N.; Cannizzaro, C.; Gerecht, S.; Elvassore, N.; Vunjak-Novakovic, G., Electrical stimulation of human embryonic stem cells: cardiac differentiation and the generation of reactive oxygen species. *Experimental cell research* **2009,** *315* (20), 3611-3619.

83. Arai, K. Y.; Nakamura, Y.; Hachiya, Y.; Tsuchiya, H.; Akimoto, R.; Hosoki, K.; Kamiya, S.; Ichikawa, H.; Nishiyama, T., Pulsed electric current induces the differentiation of human keratinocytes. *Molecular and cellular biochemistry* **2013,** *379* (1-2), 235-241.

84. Kang, S. K.; Shin, I. S.; Ko, M. S.; Jo, J. Y.; Ra, J. C., Journey of mesenchymal stem cells for homing: strategies to enhance efficacy and safety of stem cell therapy. *Stem Cells Int.* **2012,** *2012*, 342968.

85. Hwang, S. J.; Song, Y. M.; Cho, T. H.; Kim, R. Y.; Lee, T. H.; Kim, S. J.; Seo, Y.-K.; Kim, I. S., The implications of the response of human mesenchymal stromal cells in three-dimensional culture to electrical stimulation for tissue regeneration. *Tissue Eng., Part A* **2011,** *18* (3-4), 432-445.

86. Sheikh, I.; Tchekanov, G.; Krum, D.; Hare, J.; Djelmami-Hani, M.; Maddikunta, R.; Mortada, M. E.; Karakozov, P.; Baibekov, I.; Hauck, J., Effect of electrical stimulation on arteriogenesis and angiogenesis after bilateral femoral artery excision in the rabbit hind-limb ischemia model. *Vascular and endovascular surgery* **2005,** *39* (3), 257-265.

87. Alev, C.; Ii, M.; Asahara, T., Endothelial progenitor cells: a novel tool for the therapy of ischemic diseases. *Antioxid. Redox Signaling* **2011,** *15* (4), 949-965.

88. Rehman, J.; Li, J.; Orschell, C. M.; March, K. L., Peripheral blood "endothelial progenitor cells" are derived from monocyte/macrophages and secrete angiogenic growth factors. *Circulation* **2003,** *107* (8), 1164-1169.

89. Urbich, C.; Dimmeler, S., Endothelial progenitor cells. *Circulation research* **2004,** *95* (4), 343-353.

90. Cai, L.; Johnstone, B. H.; Cook, T. G.; Tan, J.; Fishbein, M. C.; Chen, P. S.; March, K. L., IFATS Collection: Human Adipose Tissue-Derived Stem Cells Induce Angiogenesis and Nerve Sprouting Following Myocardial Infarction, in Conjunction with Potent Preservation of Cardiac Function. *Stem Cells* **2009,** *27* (1), 230-237.

91. Vu, N. B.; Le, H. T.-N.; Dao, T. T.-T.; Phi, L. T.; Phan, N. K.; Ta, V. T., Allogeneic Adipose-Derived Mesenchymal Stem Cell Transplantation Enhances the Expression of Angiogenic Factors in a Mouse Acute Hindlimb Ischemic Model. Springer US: Boston, MA, pp 1-17.

92. Tateishi-Yuyama, E.; Matsubara, H.; Murohara, T.; Ikeda, U.; Shintani, S.; Masaki, H.; Amano, K.; Kishimoto, Y.; Yoshimoto, K.; Akashi, H., Therapeutic angiogenesis for patients with limb ischaemia by autologous transplantation of bone-marrow cells: a pilot study and a randomised controlled trial. *Lancet* **2002,** *360* (9331), 427-435.

93. Baldari, S.; Di Rocco, G.; Piccoli, M.; Pozzobon, M.; Muraca, M.; Toietta, G., Challenges and Strategies for Improving the Regenerative Effects of

Mesenchymal Stromal Cell-Based Therapies. *Int. J. Mol. Sci.* **2017,** *18* (10), 2087.

94. Squillaro, T.; Peluso, G.; Galderisi, U., Clinical trials with mesenchymal stem cells: an update. *Cell Transplant.* **2016,** *25* (5), 829-848.

95. Trounson, A.; McDonald, C., Stem cell therapies in clinical trials: progress and challenges. *Cell Stem Cell* **2015,** *17* (1), 11-22.

96. Assmus, B.; Honold, J.; Schächinger, V.; Britten, M. B.; Fischer-Rasokat, U.; Lehmann, R.; Teupe, C.; Pistorius, K.; Martin, H.; Abolmaali, N. D., Transcoronary transplantation of progenitor cells after myocardial infarction. *N. Engl. J. Med.* **2006,** *355* (12), 1222-1232.

97. Bhang, S. H.; Cho, S.-W.; La, W.-G.; Lee, T.-J.; Yang, H. S.; Sun, A.-Y.; Baek, S.-H.; Rhie, J.-W.; Kim, B.-S., Angiogenesis in ischemic tissue produced by spheroid grafting of human adipose-derived stromal cells. *Biomaterials* **2011,** *32* (11), 2734-2747.

98. Deuse, T.; Peter, C.; Fedak, P. W.; Doyle, T.; Reichenspurner, H.; Zimmermann, W. H.; Eschenhagen, T.; Stein, W.; Wu, J. C.; Robbins, R. C., Hepatocyte growth factor or vascular endothelial growth factor gene transfer maximizes mesenchymal stem cell–based myocardial salvage after acute myocardial infarction. *Circulation* **2009,** *120* (11 suppl 1), 247-254.

99. Madonna, R.; Taylor, D. A.; Geng, Y.-J.; De Caterina, R.; Shelat, H.; Perin, E. C.; Willerson, J. T., Transplantation of mesenchymal cells rejuvenated by the overexpression of telomerase and myocardin promotes revascularization and tissue repair in a murine model of hindlimb ischemia. *Circ. Res.* **2013**, 902-914.

100. Jay, S. M.; Shepherd, B. R.; Bertram, J. P.; Pober, J. S.; Saltzman, W. M., Engineering of multifunctional gels integrating highly efficient growth factor delivery with endothelial cell transplantation. *FASEB J.* **2008,** *22* (8), 2949-2956.

101. Fitzpatrick, J. R.; Frederick, J. R.; McCormick, R. C.; Harris, D. A.; Kim, A.-Y.; Muenzer, J. R.; Gambogi, A. J.; Liu, J. P.; Paulson, E. C.; Woo, Y. J., Tissue-engineered pro-angiogenic fibroblast scaffold improves myocardial

perfusion and function and limits ventricular remodeling after infarction. *J. Thorac. Cardiovasc. Surg.* **2010,** *140* (3), 667-676.

102. Baek, K.; Tu, C.; Zoldan, J.; Suggs, L. J., Gene transfection for stem cell therapy. *Curr. Stem Cell Rep.* **2016,** *2* (1), 52-61.

103. Nowakowski, A.; Andrzejewska, A.; Janowski, M.; Walczak, P.; Lukomska, B., Genetic engineering of stem cells for enhanced therapy. *Acta Neurobiol. Exp.* **2013,** *73* (1), 1-18.

104. Hashim, S. N. M.; Yusof, M. F. H.; Noordin, K. B. A. A.; Kannan, T. P.; Hamid, S. S. A.; Mokhtar, K. I.; Ahmad, A., Angiogenic potential of extracellular matrix of human amniotic membrane. *Tissue Eng. Regener. Med.* **2016,** *13* (3), 211-217.

105. Seif-Naraghi, S. B.; Singelyn, J. M.; Salvatore, M. A.; Osborn, K. G.; Wang, J. J.; Sampat, U.; Kwan, O. L.; Strachan, G. M.; Wong, J.; Schup-Magoffin, P. J., Safety and efficacy of an injectable extracellular matrix hydrogel for treating myocardial infarction. *Sci. Transl. Med.* **2013,** *5* (173), 173ra25.

106. DeQuach, J. A.; Lin, J. E.; Cam, C.; Hu, D.; Salvatore, M. A.; Sheikh, F.; Christman, K. L., Injectable skeletal muscle matrix hydrogel promotes neovascularization and muscle cell infiltration in a hindlimb ischemia model. *Eur. Cells Mater.* **2012,** *23*, 400.

107. Mebarki, M.; Coquelin, L.; Layrolle, P.; Battaglia, S.; Tossou, M.; Hernigou, P.; Rouard, H.; Chevallier, N., Enhanced human bone marrow mesenchymal stromal cell adhesion on scaffolds promotes cell survival and bone formation. *Acta Biomater.* **2017,** *59*, 94-107.

108. Fearon, U.; Canavan, M.; Biniecka, M.; Veale, D. J., Hypoxia, mitochondrial dysfunction and synovial invasiveness in rheumatoid arthritis. *Nature Reviews Rheumatology* **2016,** *12* (7), 385-397.

109. Krijnen, P.; Nijmeijer, R.; Meijer, C.; Visser, C.; Hack, C.; Niessen, H., Apoptosis in myocardial ischaemia and infarction. *J. Clin. Pathol.* **2002,** *55* (11), 801-811.

110. Han, T. T. Y.; Toutounji, S.; Amsden, B. G.; Flynn, L. E., Adipose-derived stromal cells mediate in vivo adipogenesis, angiogenesis and inflammation in decellularized adipose tissue bioscaffolds. *Biomaterials* **2015,** *72*, 125-137.

111. Du, J.; Chen, X.; Liang, X.; Zhang, G.; Xu, J.; He, L.; Zhan, Q.; Feng, X.-Q.; Chien, S.; Yang, C., Integrin activation and internalization on soft ECM as a mechanism of induction of stem cell differentiation by ECM elasticity. *Proc. Natl. Acad. Sci. U. S. A.* **2011,** *108* (23), 9466-9471.

112. Swift, J.; Ivanovska, I. L.; Buxboim, A.; Harada, T.; Dingal, P. D. P.; Pinter, J.; Pajerowski, J. D.; Spinler, K. R.; Shin, J.-W.; Tewari, M., Nuclear lamin-A scales with tissue stiffness and enhances matrix-directed differentiation. *Science* **2013,** *341* (6149), 1240104.

113. Chua, L. S.; Kim, H.-W.; Lee, J. H., Signaling of extracellular matrices for tissue regeneration and therapeutics. *Tissue Eng. Regener. Med.* **2016,** *13* (1), 1-12.

114. Frisch, S. M.; Screaton, R. A., Anoikis mechanisms. *Curr. Opin. Cell Biol.* **2001,** *13* (5), 555-562.

115. Livshits, G.; Kobielak, A.; Fuchs, E., Governing epidermal homeostasis by coupling cell–cell adhesion to integrin and growth factor signaling, proliferation, and apoptosis. *Proc. Natl. Acad. Sci. U. S. A.* **2012,** *109* (13), 4886-4891.

116. Burke, A. P.; Virmani, R., Pathophysiology of acute myocardial infarction. *Med. Clin. North Am.* **2007,** *91* (4), 553-572.

117. Zhu, W.; Chen, J.; Cong, X.; Hu, S.; Chen, X., Hypoxia and serum deprivation-induced apoptosis in mesenchymal stem cells. *Stem Cells* **2006,** *24* (2), 416-425.

118. Park, J.; Kim, B.; Han, J.; Oh, J.; Park, S.; Ryu, S.; Jung, S.; Shin, J.-Y.; Lee, B. S.; Hong, B. H., Graphene oxide flakes as a cellular adhesive: prevention of reactive oxygen species mediated death of implanted cells for cardiac repair.

*ACS nano* **2015,** *9* (5), 4987-4999.

119. François, S.; El Benna, J.; Dang, P. M.; Pedruzzi, E.; Gougerot-Pocidalo, M.-A.; Elbim, C., Inhibition of neutrophil apoptosis by TLR agonists in whole blood: involvement of the phosphoinositide 3-kinase/Akt and NF-κB signaling pathways, leading to increased levels of Mcl-1, A1, and phosphorylated Bad. *J. Immunol.* **2005,** *174* (6), 3633-3642.

120. Grossmann, J.; Mohr, S.; Lapetina, E. G.; Fiocchi, C.; Levine, A. D., Sequential and rapid activation of select caspases during apoptosis of normal intestinal epithelial cells. *Am. J. Physiol.* **1998,** *274* (6), G1117-G1124.

121. Landázuri, N.; Levit, R. D.; Joseph, G.; Ortega-Legaspi, J. M.; Flores, C. A.; Weiss, D.; Sambanis, A.; Weber, C. J.; Safley, S. A.; Taylor, W. R., Alginate microencapsulation of human mesenchymal stem cells as a strategy to enhance paracrine-mediated vascular recovery after hindlimb ischaemia. *Tissue Eng. Regener. Med.* **2016,** *10* (3), 222-232.

# 요약 (국문초록)

본 연구는 쥐 하지 허혈 모델에서 태양 전지 유래의 전기 자극과 주사 가능한 탈세포화 된 세포 외 기질을 세포와 함께 이식 하는 방법을 이용하여 신생 혈관 재생 치료의 향상에 대한 것 이다. 허혈 조직에서 대부분의 이식된 세포와 원 조직의 세포는 낮은 산소 농도와 낮은 영양소 전달에 의해 사멸을 일으키게 된다. 따라서 기존의 치료 방법 대신 향상된 세포 치료 방법이나 세포를 사용하지 않는 치료법의 개발이 필요하다.

제 3장에서는 세포의 거동을 조절하고 신생 혈관 재생을 촉진 할 수 있는 세기의 전기적 에너지를 낼 수 있는 태양 전지 기반의 장치를 개발하려 쥐 하지 허혈 모델에 적용하였다. 동물 실험의 편의성을 위해 태양 전지 회로는 이식 전극과 부착 태양광 판으로 구성되었다. 기존의 전기 치료에는 큰 전기 장치가 필요로 하지만, 본 연구에서 개발 한 태

양 전지 기반의 착용 가능한 기기는 그러한 제약을 극복하여 환자가 입원하지 않고도 치료 가능하게 할 것이다. 세포에 전기 자극을 적용하였을 때, 다양한 종류의 세포에서 혈관 재생 인자가 증가하고 세포 이동능이 증가하는 것을 확인 할 수 있었다. 태양 전지를 이용한 쥐 실험에서 하지 허혈 부위에 전극을 이식하고 쥐의 등 부분에 태양 전지판을 부착하여 외부의 빛에 노출시켰다. 이러하 장치는 빛 에너지를 치료에 충분한 전기 에너지로 전환 하였으며, 혈관 재생 인자가 증가하고 하지 허혈 모델에서의 치료 효과가 증가함을 확인 할 수 있었다.

제 4장에서는 주사 가능한 탈세포화된 기질을 개발하고 이 물질이 이식된 세포의 생체 내 부착과 치료 효능을 향상시킬 수 있는지 확인하였다. 이 물질을 세포와 섞은 후 쥐 하지 허혈 모델에 적용 하였을 때 혈관 재생 인자들이 증가하고, 치료 효과가 증대 됨을 확인 할 수 있었다.

본 연구에서 개발한 전기 자극을 발생시키는 태양 전지 기기와 탈세포

화된 주사 가능한 기질은 사용이 쉽고 혈관 재생 치료에 간편하게 이용 될 수 있는 장점이 있다. 따라서 앞으로의 추가적인 연구에 따라 실제 환자의 치료에 적용 될 수 있는 가능성이 있을 것으로 예상한다.

주요어 : 혈관신생, 허혈 질환, 줄기세포 이식, 태양 전지, 탈세포화 기질, 세포 외 기질

학번 : 2012-20973